The 'meat': Biogeochemical inversions

1. To obtain concentration.
2. To obtain information on the size distribution.
3. To obtain composition information.
4. To obtain rate of processes .

Inversions to obtain concentrations

- Chlorophyll a
- TPV
- TSM (SPM)
- POC
- DOC

Not covered: new optical inversions to obtain nitrate and oxygen based on effect on UV absorption.

Inversions to obtain chlorophyll concentration

Question: why do we want to know [chl]?

- For biomass we want C_{phyto}.
- For primary production we need a_{ϕ}.

We are hooked on [chl] because:

- It is specific to phytoplankton.
- It is easy to measure.
- It has been historically measured a lot.

Methodological issues associated with biogeochemical measurement:

- Potential for interference from other pigments when the laboratory based fluorometric method is used.
- Replication.

Obtainint [chl] using the red peak absorption of the ac-9:

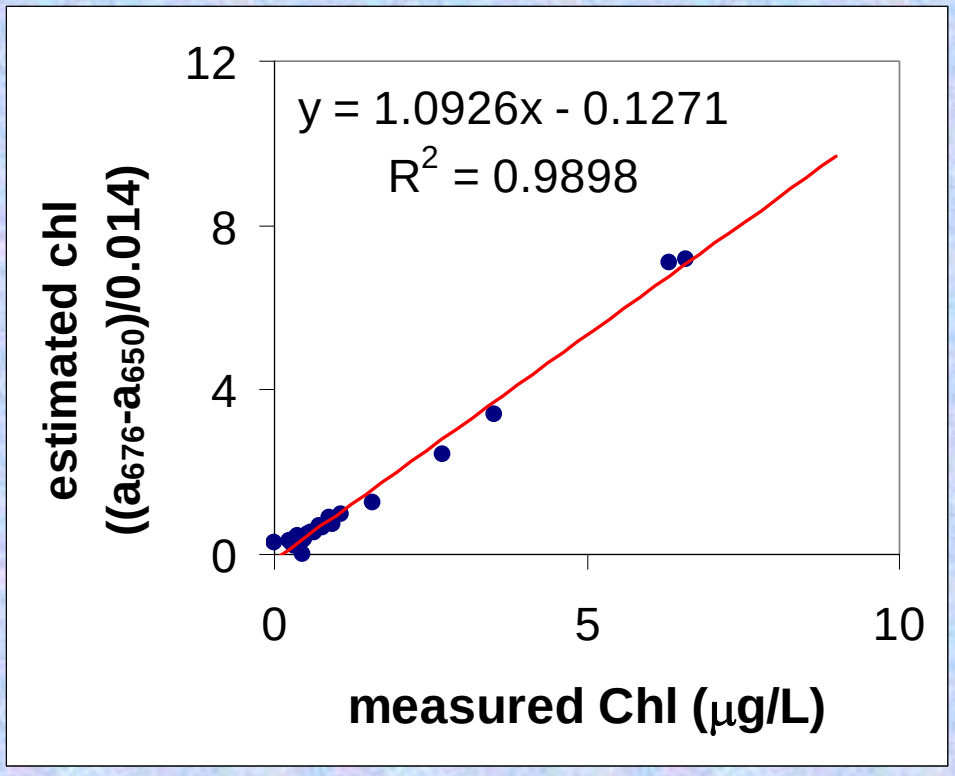

Karp-Boss, 2001, unpublished

Variations on: $[chl]=a_{\phi}/a^*$

Problems:

1. Packaging at 676nm -0.03>a*>0.008 m^2/mg chl
2. other pigments absorbing in that region.

Advantage: absorption is dominated by phyto.

Another issue with correlations:
R^2 is not a good predictor of uncertainty in estimated parameter. Dominated by dynamic range.

Obtaining [Chl] with in-situ fluorescence (blue→red):

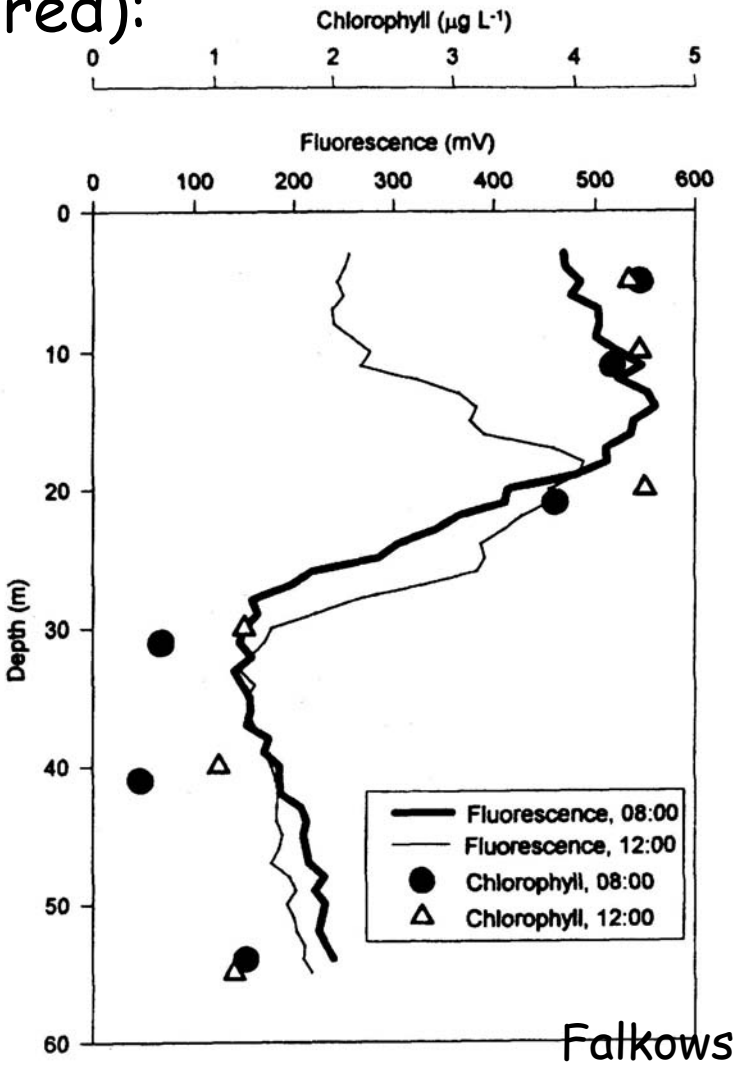

Falkowski and Raven, 1997

Figure 9.6 An example of nonphotochemical quenching of in vivo fluorescence in the ocean. An in situ fluorometer, with a xenon flash excitation source, was lowered from the surface to 55 m at 0800 and 1200 hours local time in the northwestern Atlantic in April. The fluorescence intensity was shown in real time on the deck of the ship and recorded in engineering units as a voltage. During the vertical profile, water samples from discrete depths were obtained and the chlorophyll *a* was extracted in 90% acetone and analyzed independently. A comparison of the in vivo fluorescence profiles between early morning and midday reveals a sharp decrease in the fluorescence intensity in the upper 20 m that is not reflected in the extracted chlorophyll analyses.

Problem: quantum yield of fluorescence (photon fluoresced per photon absorbed) is variable with **light history** (NPQ) and **species**.

Advantage: fluorescence comes from the photosynthetic machinery (but only from one PS).

Obtaining chl from reflectance ratios:

From: http://oceancolor.gsfc.nasa.gov/ocproducts.html

The SeaWiFS Chlorophyll a concentration

OC4v4 (SeaWiFS):

$$C_a = 10^{0.366 - 3.067R + 1.930R^2 + 0.649R^3 - 1.532R^4}, \text{ where } R = log_{10}\left(\frac{R_{rs}443 > R_{rs}490 > R_{rs}510}{R_{rs}555}\right)$$

OC4v4 Makes use of a maximum band-ratio that incorporates 443, 490 and 510 nm

Level 2 metadata
chlor_a:slope = 1
chlor_a:intercept = 0

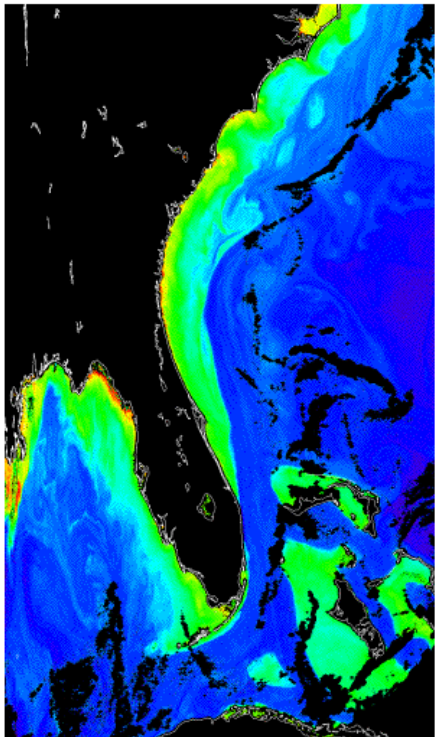

The Chlorophyll a concentration

OC3M MODIS chlor_a:

$$C_a = 10.0^{(0.2830 - 2.753R_{3M} + 1.457R_{3M}^2 + 0.659R_{3M}^3 - 1.403R_{3M}^4)}$$
where $R_{3M} = \log_{10}(R_{550}^{443} > R_{550}^{490})$

Scale = log10
Range = 0.015 -2.0 0 - 64 mg m-3

•OC3 incorporates 443 and 488
•As turbidity increases, the maximum band migrates from blue to green.
•Seawifs utilizes OC4 - differences between SeaWiFS and MODIS chlor can approach 25% in turbid waters.

Level 2 metadata
chlor_a: slope = 1
chlor_a: intercept = 0

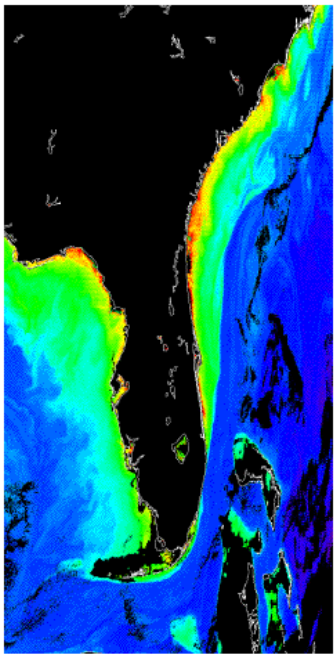

Some data about uncertainties:

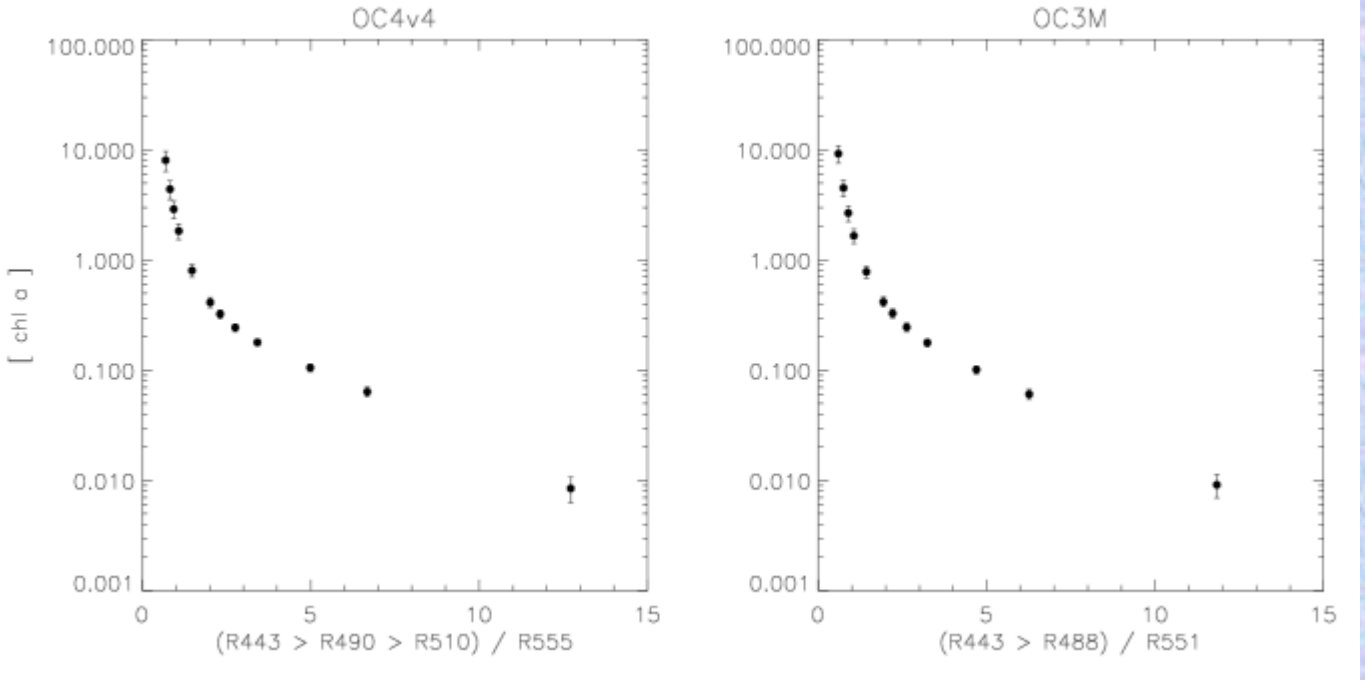

potential [chl] difference for 5% error in input Rrs

Input chl	10	5	3	2	1	0.5	0.4	0.3	0.2	0.1	0.05	0.01
OC4V4 %diff	21	19	18	16	13	10	9	8	7	8	10	26
OC3M %diff	18	17	16	15	13	10	10	8	8	8	11	24

From: http://seabass.gsfc.nasa.gov/eval/oc.cgi

Problem: how do we know that the data we are interested in is similar to the training set?

Inversions to obtain TPV, TSM and POC

Question: why do we want to know POC, TPV or TSM?

- Carbon pool

- Sediment studies

Methodological issues associated with biogeochemical measurement:

- Filtration between dissolved and particulate.
- Upper size filtration-zooplankton.
- Filtered volume.
- Salts.
- Replication.

Obtaining TPV from Beam-c (660):

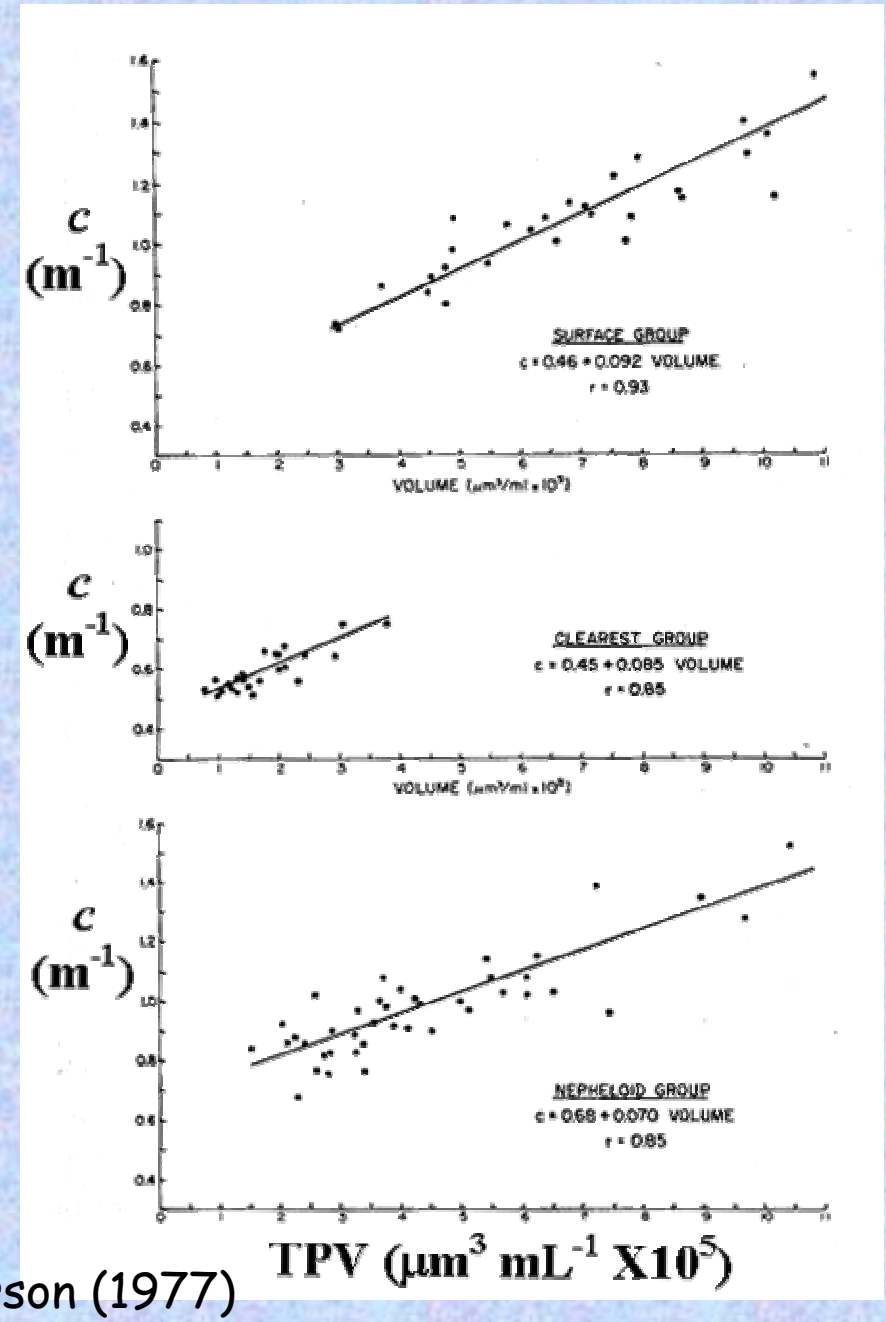

Peterson (1977)

Likely causes for variability: PSD, composition, Particles not accounted by sizing device, non-sphericity.

Spinrad et al. (1983):

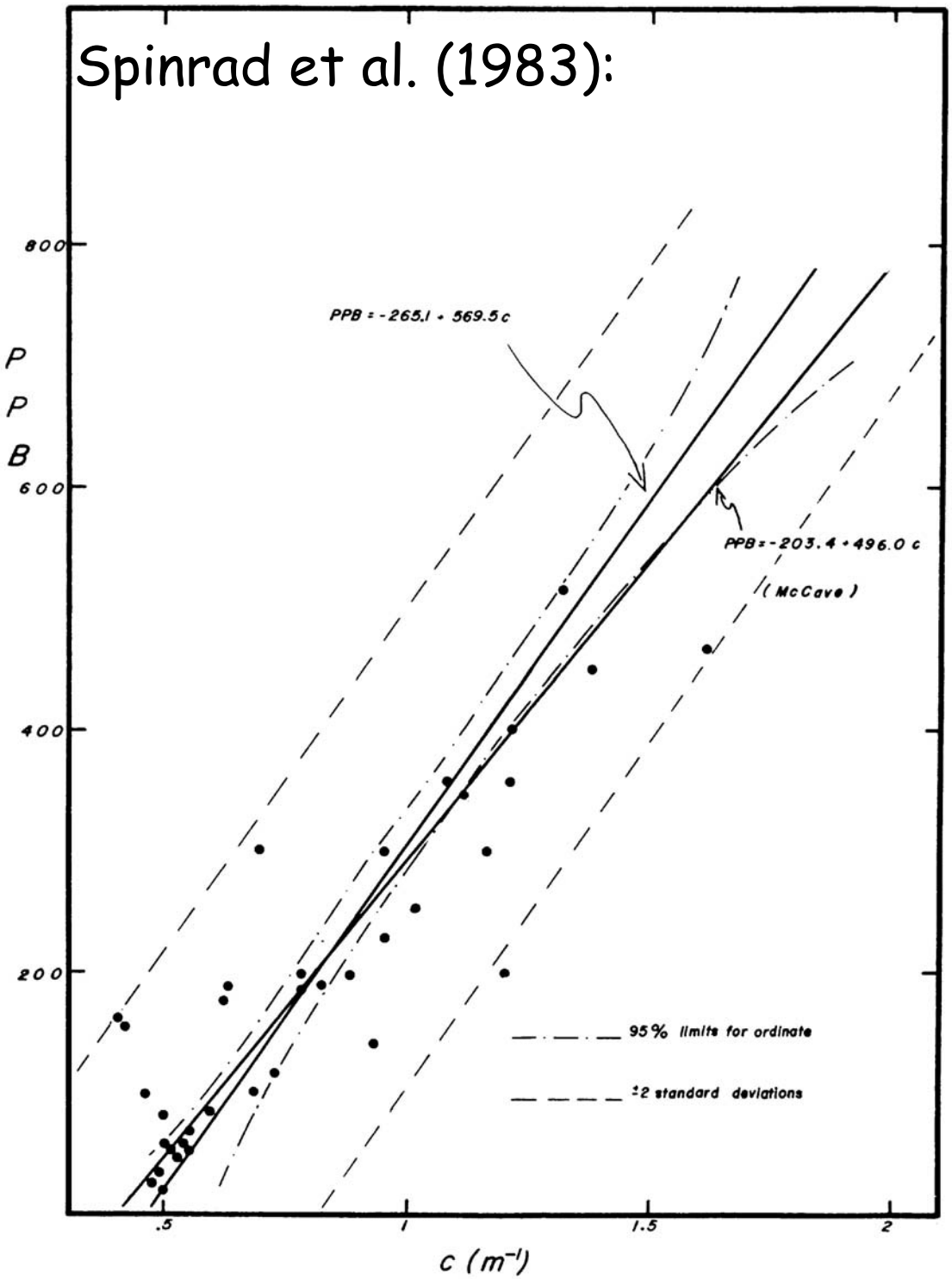

2. Correlation of particle volume concentration (ppb = parts per billion) and beam attenuation coefficient.

Deep ocean

Obtaining SPM from $b_p(555)$:

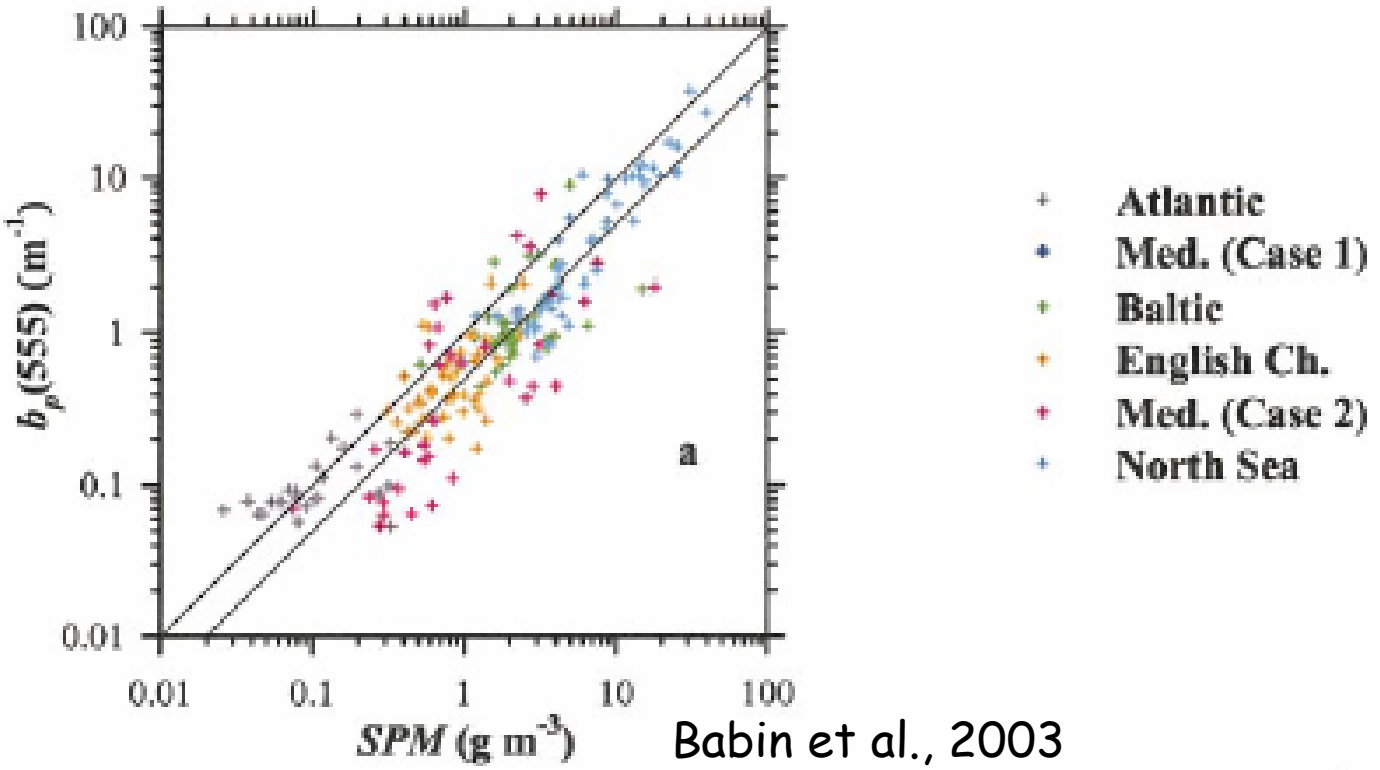

Babin et al., 2003

Table 4. Overall and site-by-site statistics of the $b_p(555)$: SPM ratio. Normality of distributions was verified successfully using a Komolgorov–Smirnov test on log-transformed data. The geometric standard deviation (SD) is to be applied as a factor. Averages were compared between regions using a Fisher PLSD test. They were considered as significantly different when $p < 0.0005$. The column "Different from regions (ID)" shows the regions identified through ID, which are significantly different from a given region listed in the region column. No SPM data were collected in Med. (case 1). Note that only samples for which scattering data were available are considered. No. is the number of observations.

ID	Region	No.	Average (m^2 g^{-1})	SD	Different from regions (ID) ($p < 0.0005$)
a	Atlantic	25	0.97	1.9	c, d, e, f
b	Med. (case 1)	—	—	—	—
c	Baltic	44	0.49	1.7	a
d	Channel	46	0.56	1.7	a
e	Med. (case 2)	35	0.42	2.6	a
f	North sea	55	0.54	1.6	a
—	All case 2	180	0.51	1.9	—

$b_p(555)^* \sim 0.5 m^2/g$

How can it work for both organic and inorganic particles?

Aside: example of size effect on scattering:

LSS

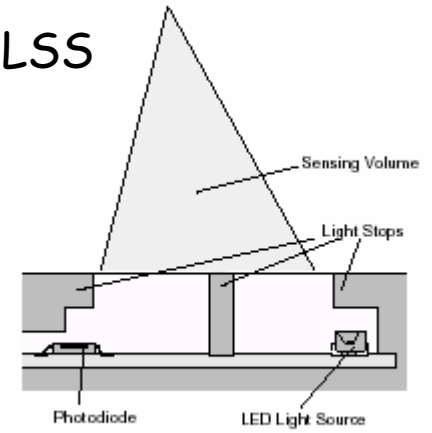

Figure 2. Diagram of Seapoint Turbidity Meter Optics

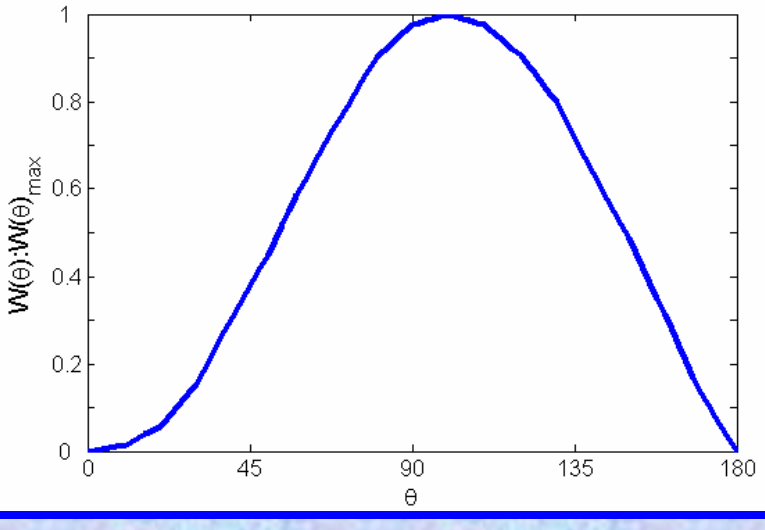

Response of the LSS to size (Baker et al., 2001):

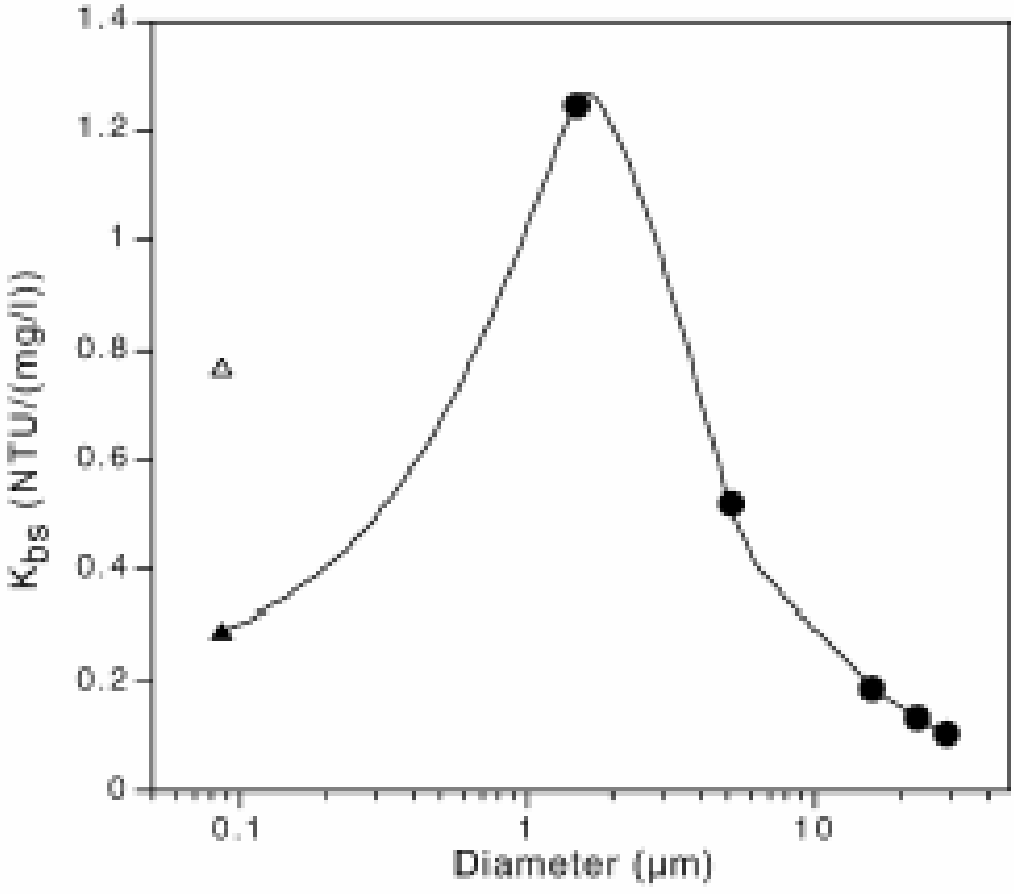

Obtaining POC from Beam-c (660):

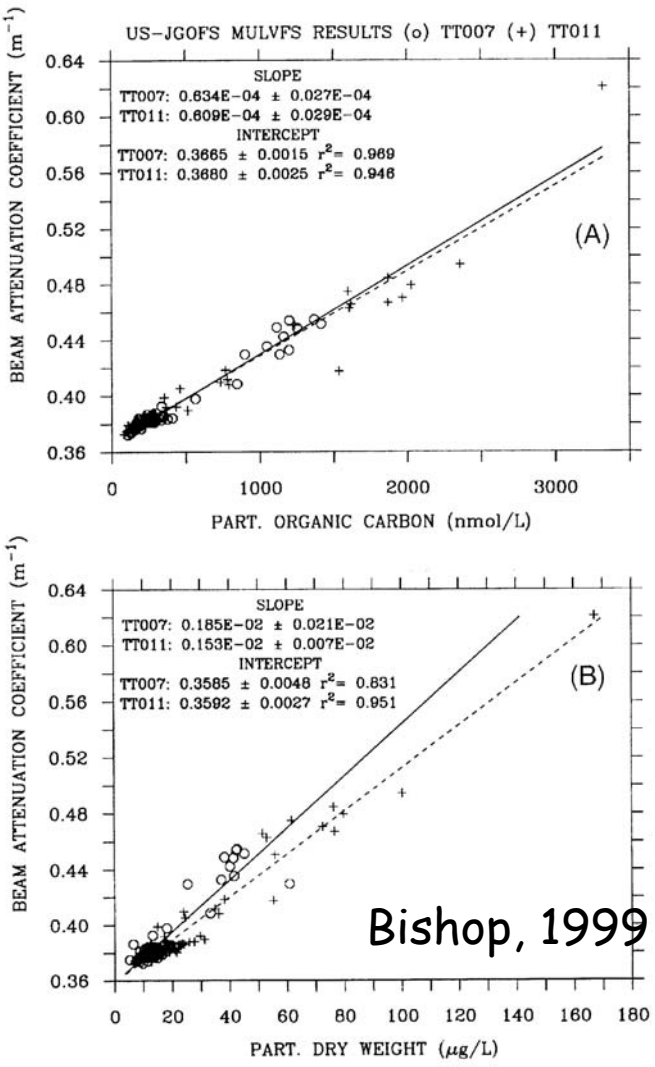

Bishop, 1999

Fennel and Boss, 2003:

Table 1. Our regression $c_p = a\mathrm{POC} + b$ in comparison with other published relationships.

Location	Slope a [m^{-1}(mmol C m^{-3})$^{-1}$]	Intercept b (m^{-1})
Station ALOHA (present study)	0.019	−0.006
Equatorial Pacific (Bishop 1999)	0.006	0.010*
Subarctic Pacific (Bishop et al. 1999)	0.006	0.005*
Arabian Sea (Gunderson et al. 1998)†	0.031	−0.007
Southern Ocean (Gardner et al. 2000)†	0.019	0.010

* Published relationship contains attenuation component due to water. For this comparison, 0.358 m^{-1} was subtracted

† Independent relationships were determined for different cruises. Values are given for the summer cruise in the Southern Ocean and the late north-eastern monsoon period in the Arabian Sea.

Likely causes for variability: PSD, composition, Particles not accounted by POC method.

Obtaining POC from Beam-c (660):

SOLO float-
Carbon explorers:

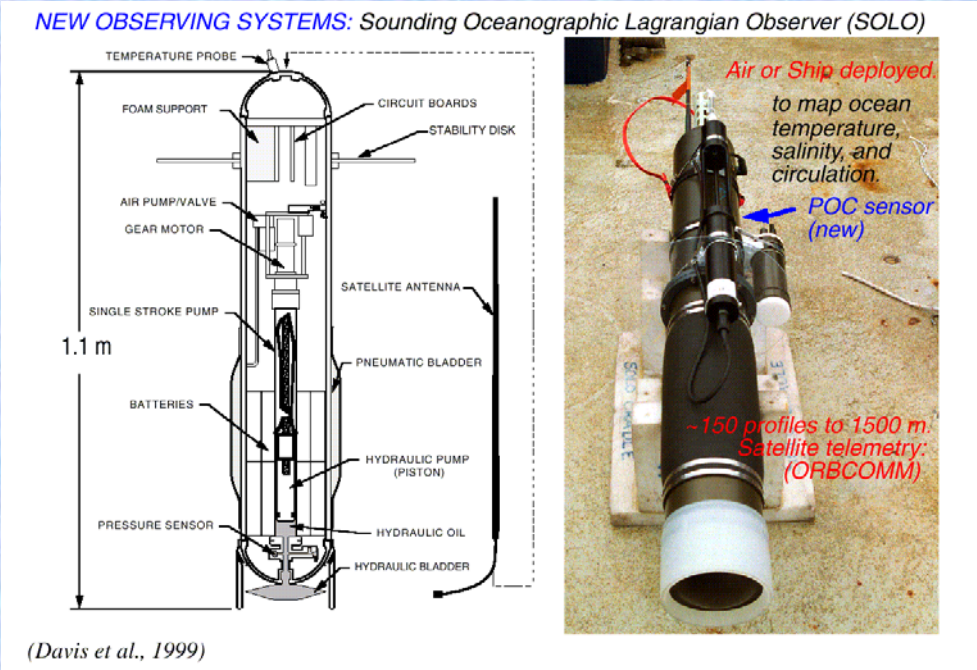

Results:

Two blooms of phytoplankton in North Pacific following dust deposition event (iron fertilization ?).

SeaWIFS [chl] and POC covary.

Notice co-variation of blooms and stratification and high chl/C ratios (vernal bloom ?).

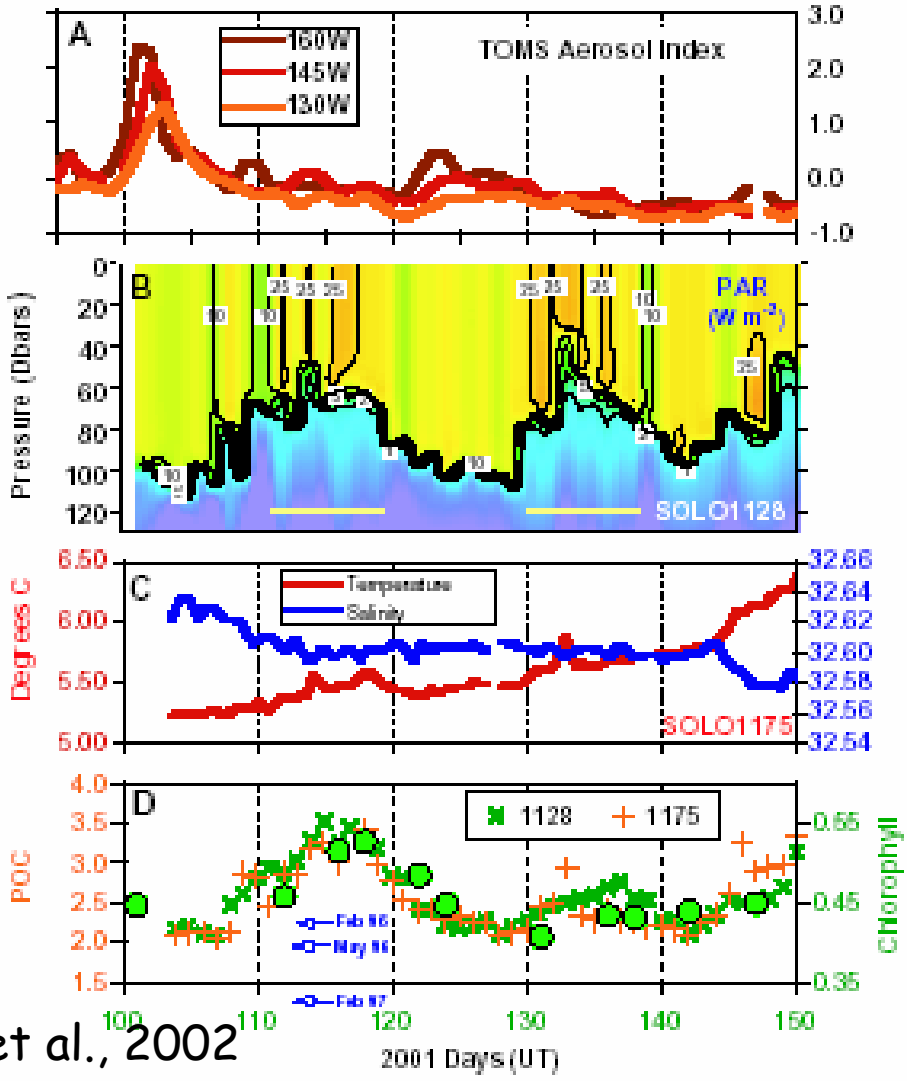

Bishop et al., 2002

Obtaining POC from $b_{bp}(510)$:

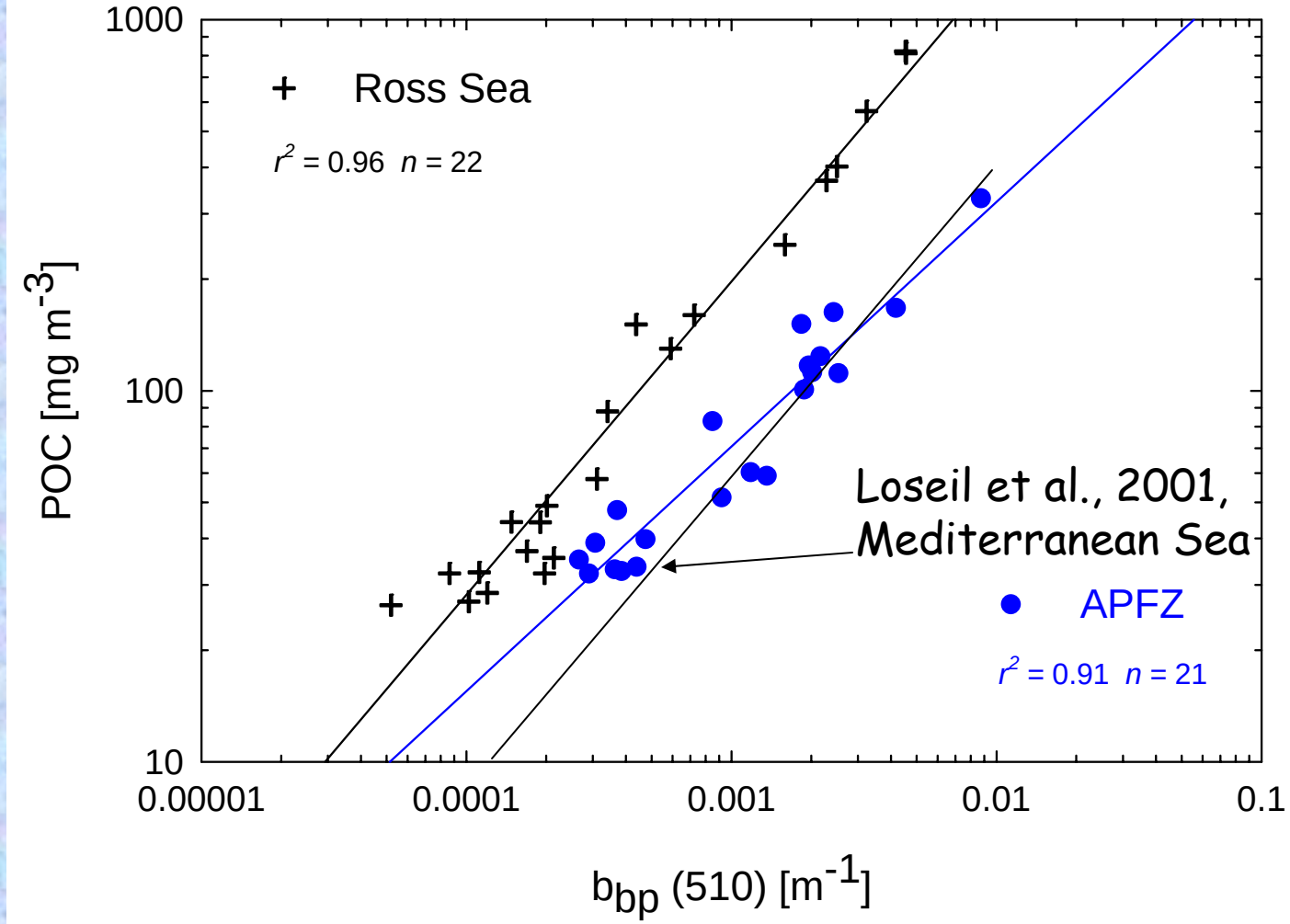

Stramski et al, 1999.

Likely causes for variability: b_{bp} computation, PSD, composition, Particles not accounted by POC method.

Loseil et al., 2001: b_{bp} from Ocean color.
Stramski et al., 1999: in-situ b_{bp}.

Can we get C_{phyto} from optical proxies?

How much of POC is C_{phyto}?

The few (4) studies who looked at it (with variable methods) suggest it varies from 19-50%.

However, within studies the variability is much smaller:

Oubelkheir found the variability between oligotrophic, mesotrophic and eutrophic C_{phyto}/POC to vary from 19-22%.

Durand et al., 2001, comparing seasons at BATS from Cphyto/POC to be nearly constant across seasons.

The time variable part of POC that correlates with the T, N and/or E_d is likely to be correlated with phytoplankton. Micro-grazers and bacteria can grow as fast as phytoplankton.

➔This very limited set of observations suggest that measurements of scattering may provide a useful proxy for C_{phyto}.

Inversions to obtain a_ϕ

a_ϕ is an important input to primary production models.

It is more directly related to ocean color than [chl].

Obtaining a_ϕ from $R_{rs}(\lambda)$ and $k(\lambda)$:

Using semi-empirical relationships:

$$R_{rs}(\lambda) = G(\lambda)\frac{b_b(\lambda)}{a(\lambda)+b_b(\lambda)}, \quad k_d(\lambda) = \frac{a(\lambda)+b_b(\lambda)}{\mu(\lambda)}$$

Assume spectral shapes for components of b_b and a.

$$a(\lambda) = a_{sw}(\lambda,T) + a_g(\lambda_0)\cdot\tilde{a}_g(\lambda) + a_{NAP}(\lambda_0)\cdot\tilde{a}_{NAP}(\lambda) + a_\phi(\lambda_0)\cdot\tilde{a}_\phi(\lambda)$$

$$b_b(\lambda) = b_{bsw}(\lambda) + b_{bp}(\lambda_0)\tilde{b}_{bp}(\lambda)$$

Assume water IOPs are known, $G(\lambda)$ and $\mu(\lambda)$=const., assume spectral shapes to the unknown IOPs, and best-fit (e.g. least-squares) the observed $R_{rs}(\lambda)$ and $k(\lambda)$ to solve for the amplitudes.

For the observations $Y(\lambda_i)$ assume a model $y(\lambda_i,a)$. Minimize:

$$\tilde{\chi}^2 = \sum_{i=1}^{N}\left(\frac{Y(\lambda_i) - y(\lambda_i;\mathrm{a})}{\sigma_i}\right)^2$$

A more *robust* approach; minimize

$$\tilde{\chi} = \sum_{i=1}^{N} \left| \frac{Y(\lambda_i) - y(\lambda_i; \mathrm{a})}{\sigma_i} \right|$$

Press et al., Numerical Recipes:

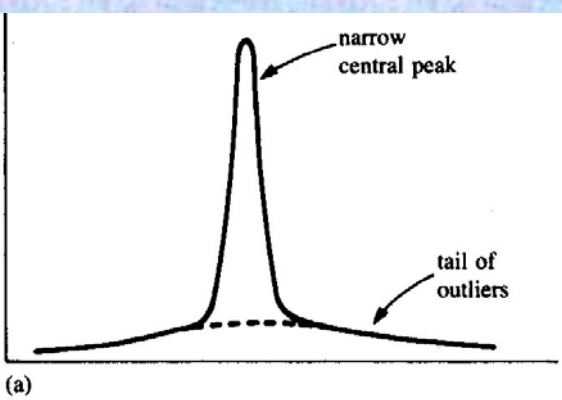

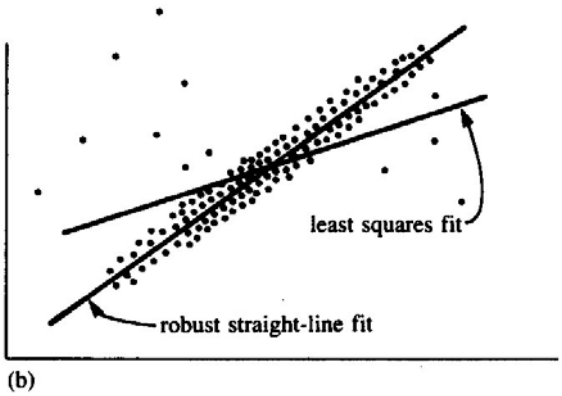

Figure 14.6.1. Examples where robust statistical methods are desirable: (a) A one-dimensional distribution with a tail of outliers; statistical fluctuations in these outliers can prevent accurate determination of the position of the central peak. (b) A distribution in two dimensions fitted to a straight line; non-robust techniques such as least-squares fitting can have undesired sensitivity to outlying points.

Example: Brown et al., 2004, measurements from an AUV:

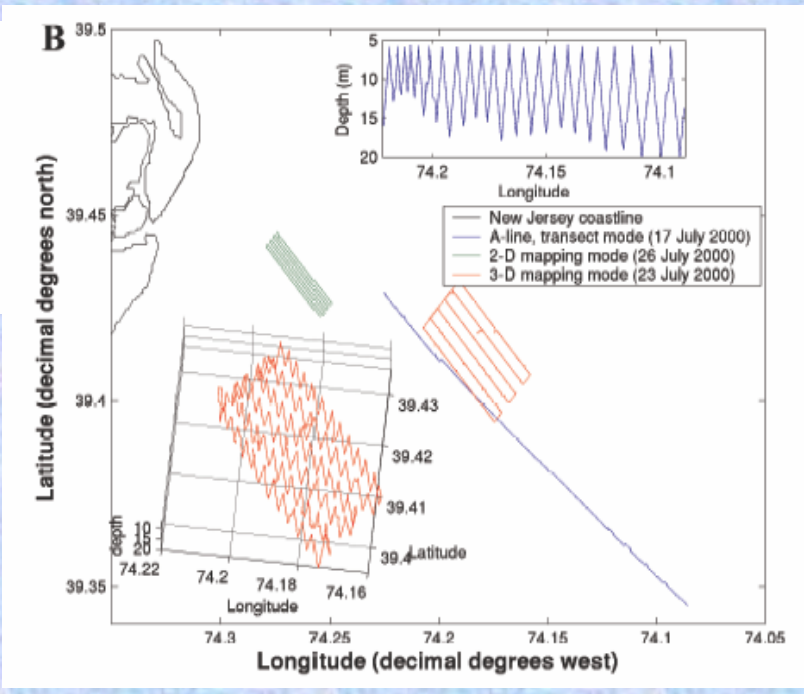

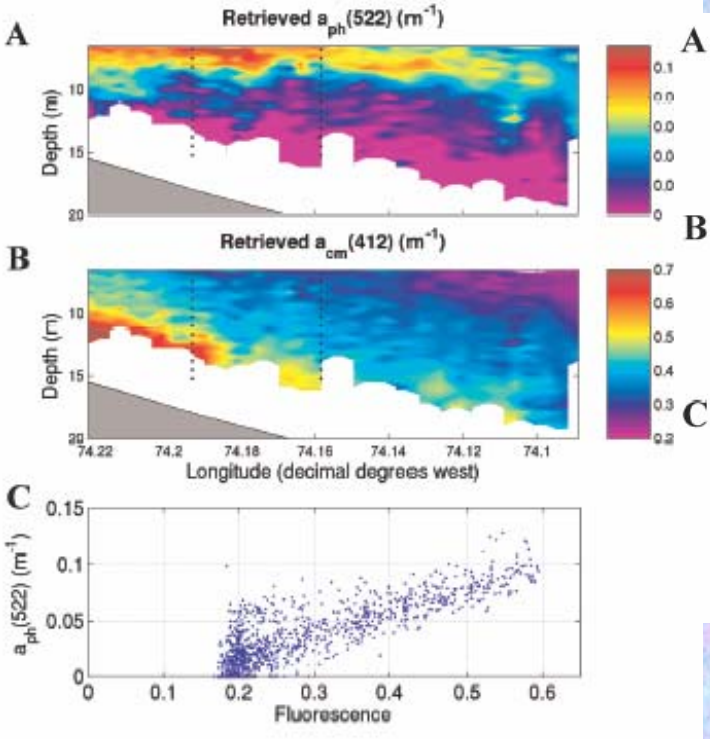

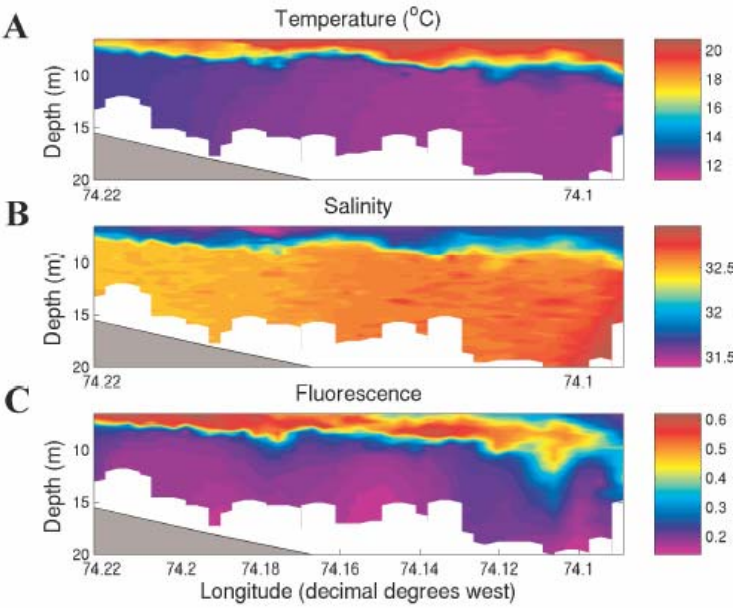

Particulate size distribution

Particle size distribution (PSD):

Most often used is the power-law, or 'Junge-like' function:

$$N(D)dD = N_o(D/D_o)^{-\xi}$$

How does attenuation changes with changes in PSD?

$$c(\lambda) = \frac{\pi}{4}\int_{D_{\min}}^{D_{\max}} C_{ext}(n, n', D, \lambda) N(D) dD$$

$N(D)dD=N_o(D/D_o)^{-\xi}$

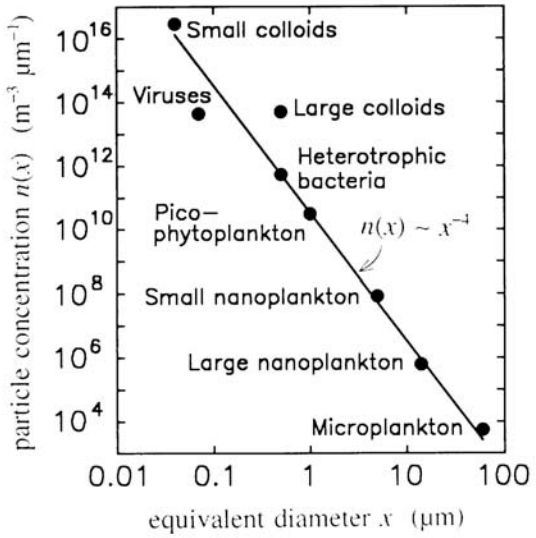

Fig. 3.2. Number size distribution typical of biological particles in the open ocean. [figure courtesy of D. Stramski]

Typically, $2.5<\xi<5$
Most frequently $3.5<x<4$

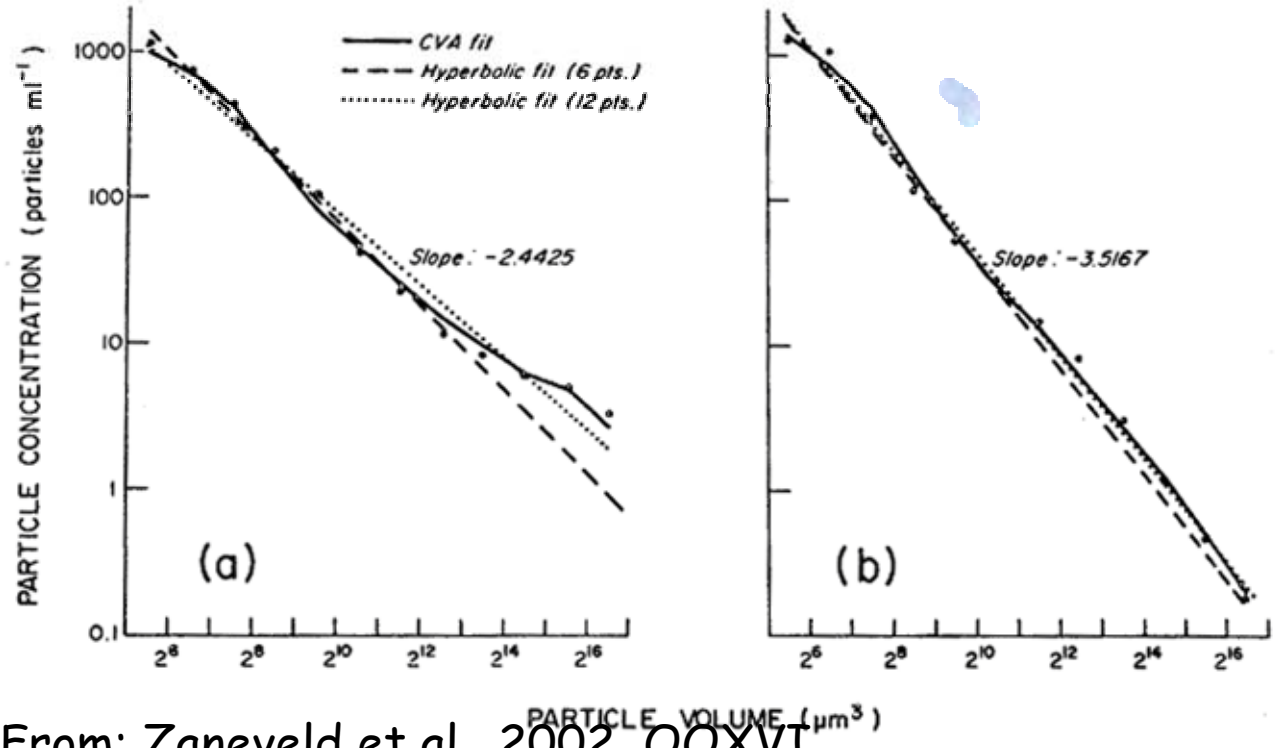

From: Zaneveld et al., 2002, OOXVI.
Data from Kitchen (1977).
CVA= characteristic vector analysis (2 vectors).

Using $c_p(\lambda)$ to obtain information on PSD:

Mie Theory (homogenous spheres):

For non-absorbing particles of the same *n* and an hyperbolic distribution from $D_{min}=0$ to $D_{max}=\infty$,

$$N(D)=N_o(D/D_o)^{-\xi}$$

$$c_p(\lambda)=c_p(\lambda_0)\left(\frac{\lambda}{\lambda_0}\right)^{-\gamma},\ \xi=\gamma+3$$

→ expect a relation between attenuation spectrum and PSD.

$c_p(\lambda)$ is sensitive to the PSD,

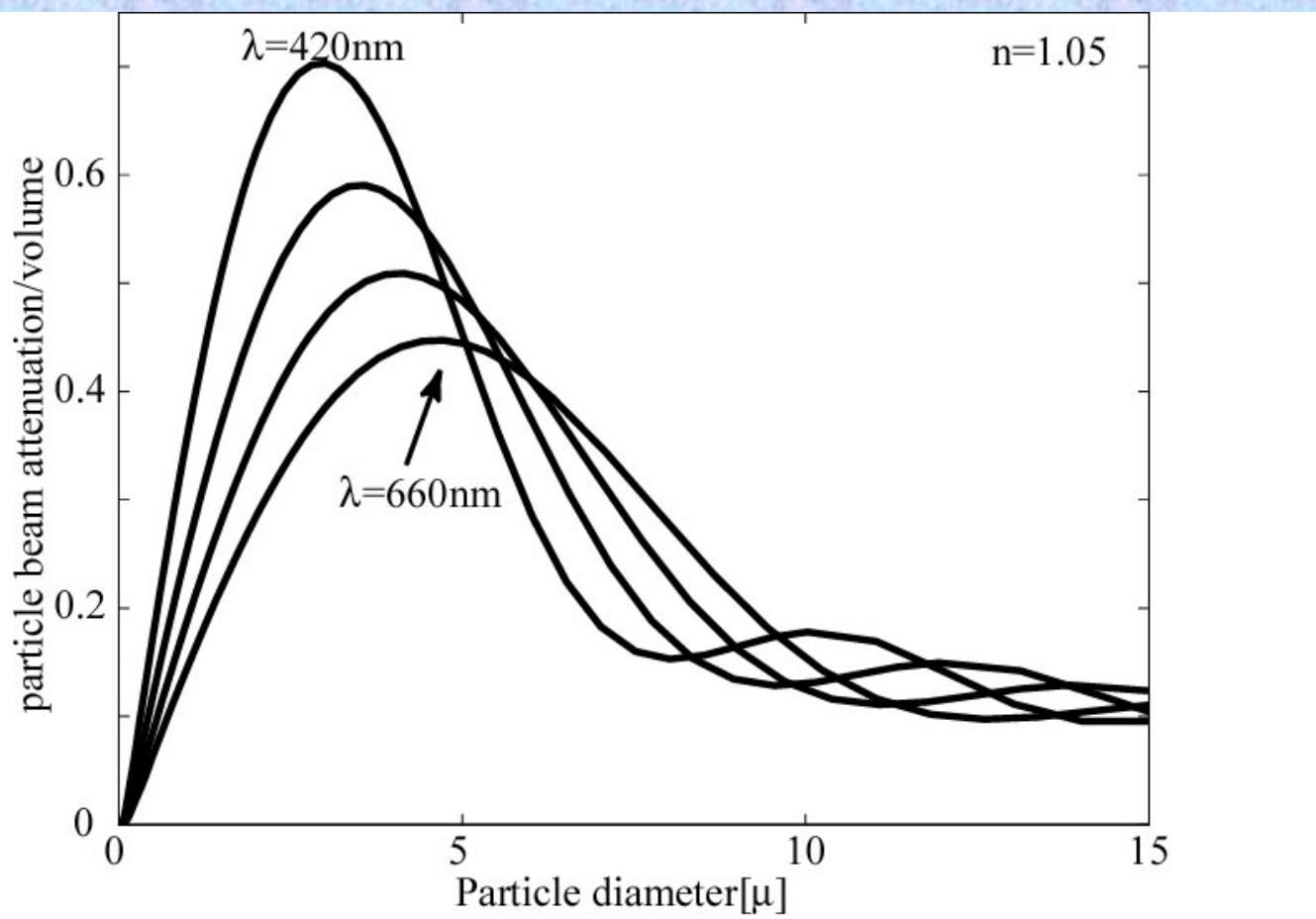

Because the instrumental 'filter' is size dependent:

- Particle size where maximum occurs changes by ~ 2 between blue to red wavelengths.
- Magnitude and width of maximum change with λ.

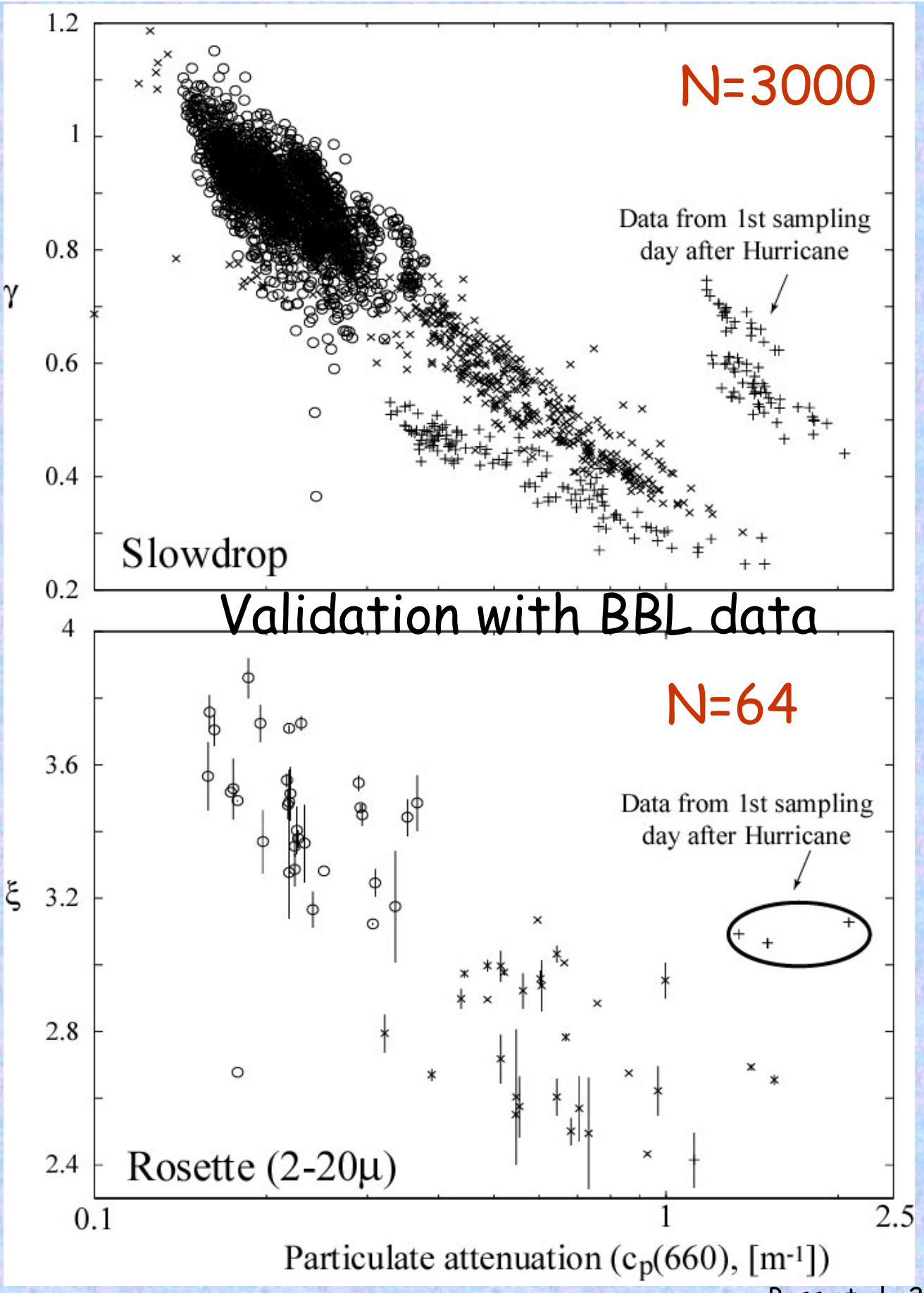

Boss et al., 2001

Observations:

- Both ξ and γ decrease monotonically with decreasing attenuation.

- Theoretical and observed relationship between ξ and γ are within 30% of ξ, despite the potentially large uncertainties associated with the sampling methods.

- Better agreement with modified theory: $\gamma \geq 0$ in observation for $\xi<3$.

- Supports the use of γ as a tool to estimate the PSD slope. In the least, it describes the changes in the mean particle diameter (proportion of big vs. small).

Particulate size distribution from the VSF:

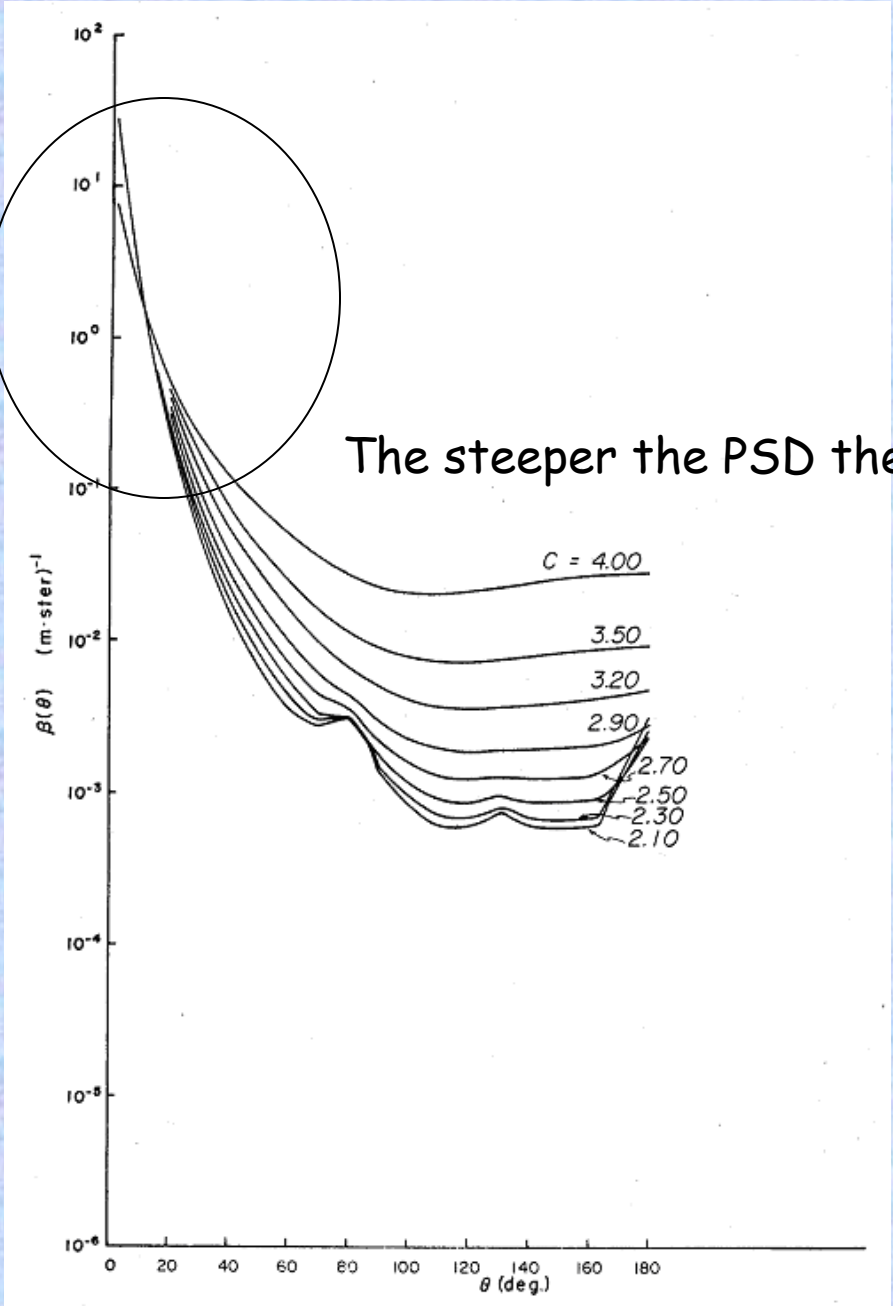

The steeper the PSD the steeper is β

Normalized volume scattering functions for various particle size distributions characterized by the cumulative 'Junge' exponent C, with a refractive index 1.075 (Roach, 1974).

Less sensitive to *n* (see IOP lecture).

PSD from near forward VSF -- LISST

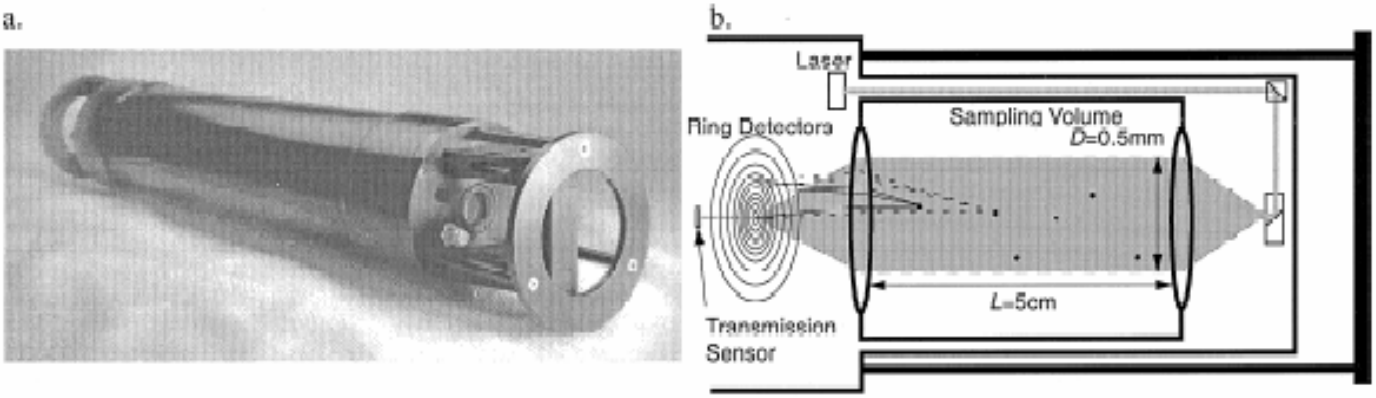

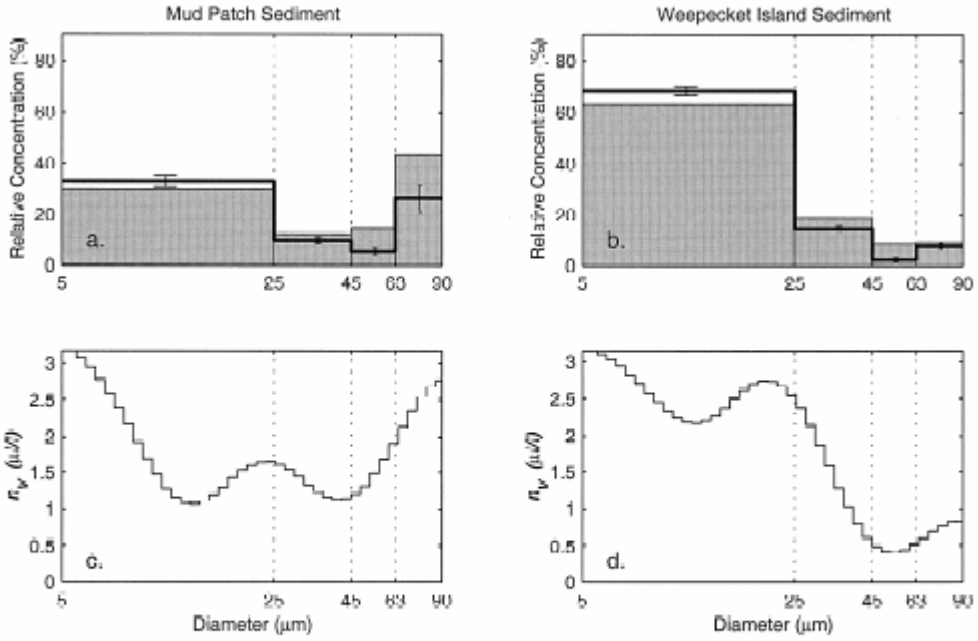

Fig. 7. Volumetric size distribution of natural sediments from The New England shelf mud patch (plots a and c) and Weepecket Island plot (b and d). In the upper plots the shaded areas indicate the relative (percent of total sample weight) mass distribution as retained in the sieves and the solid line is the relative (percent of total volume) LISST volumetric size distribution integrated into the sieve size classes. Error bars are calculated by the standard deviation during the averaging period used in calculating the relative concentration The lower plots show the LISST measured volumetric size distribution n_V in the 64 logarithmically spaced LISST size bins.

Traykovski et al., 1999

See posters by Trisha Bergmann and Wayne Slade at OOXVII

Particulate composition

Index of refraction (n) from b_{bp}/b_p:

It turns out the b_{bp}/b_p is very sensitive to n and less so to the PSD:

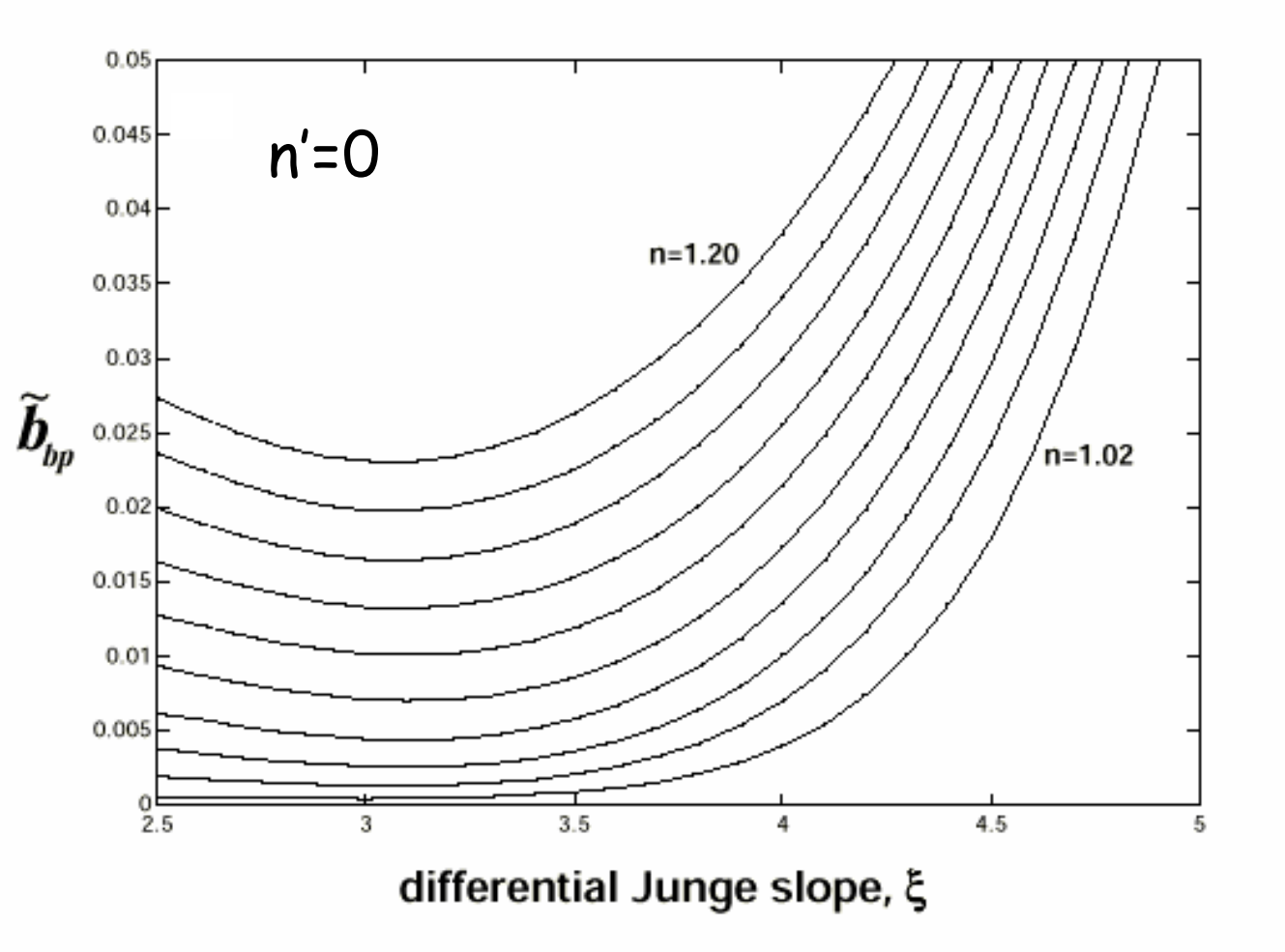

Twardowski et al., 2001

Why do we want to know *n*?

- *n* correlates with density (ρ) → sinking rates.

- *n* separates water-filled organic particles from inorganic particles.

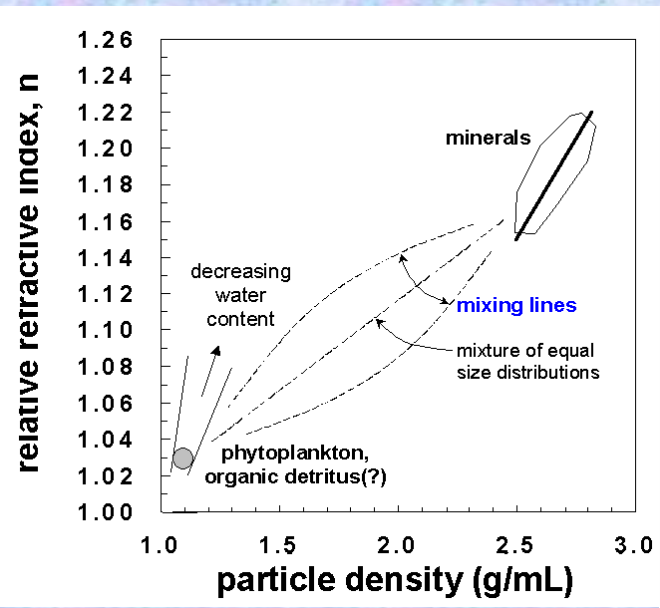

Zaneveld et al., 2002, OOXVI. Compiled from:
Aas (1983)
Carder et al. (1972)
Carder et al. (1974)

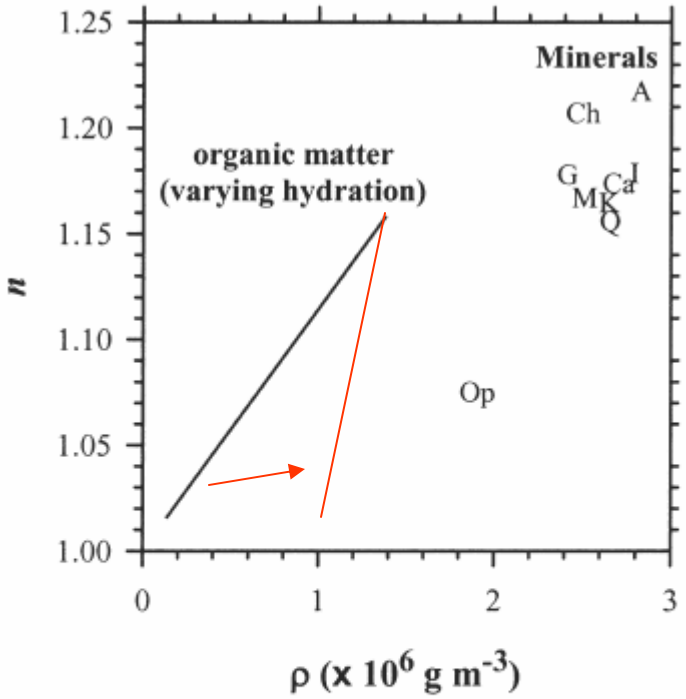

Fig. 7. The index of refraction relative to seawater for various minerals as a function of particle density. The *n* and *ρ* values (also listed in Table 6) are from Lide (2001). The *n* values are the arithmetic average of the values given for the two or three structure coordinate axes. The plotted minerals are aragonite (A), calcite (Ca), chlorite (Ch), gibbsite (G), illite (I), kaolinite (K), montmorillonite (M), opal (Op), and quartz (Q). The theoretical relationship between *n* and *ρ* is also shown for organic matter (*see text for details*).

Babin et al., 2003

Example: Leo-15, New Jersey, July 2000 {HyCODE}.

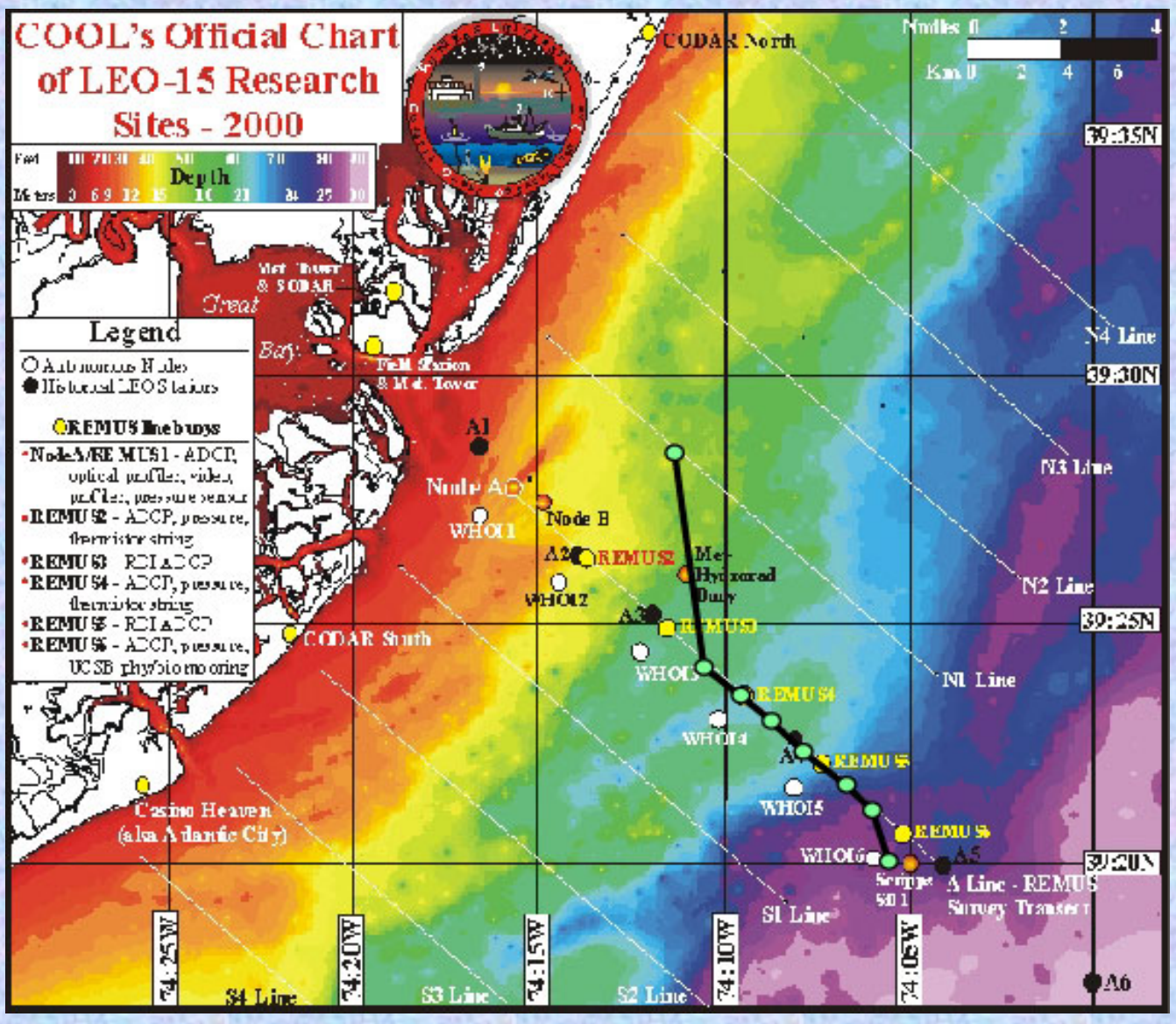

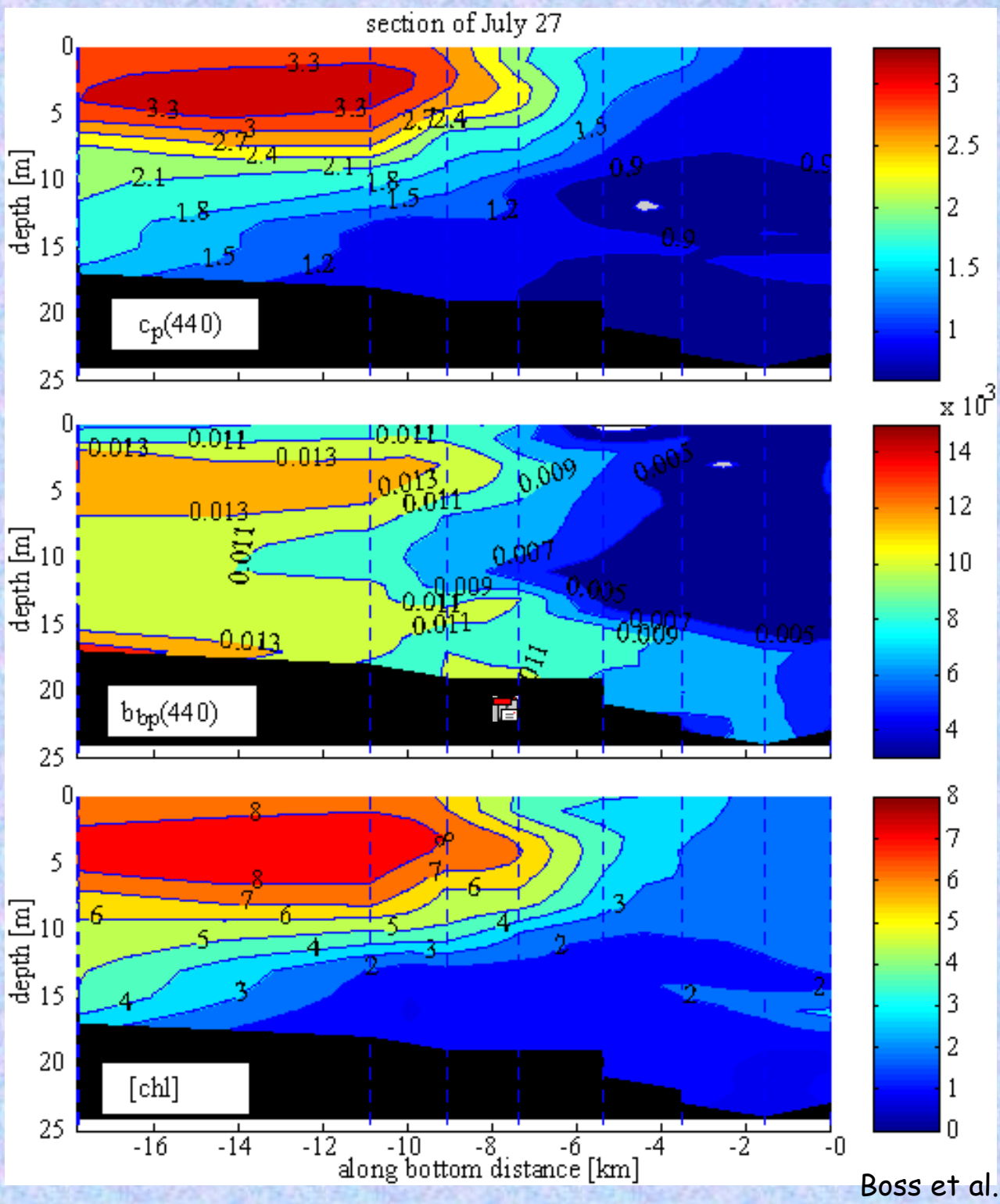

Boss et al., 200

→ b_{bp} and c_p have different informational content

Detached nephloid layer:

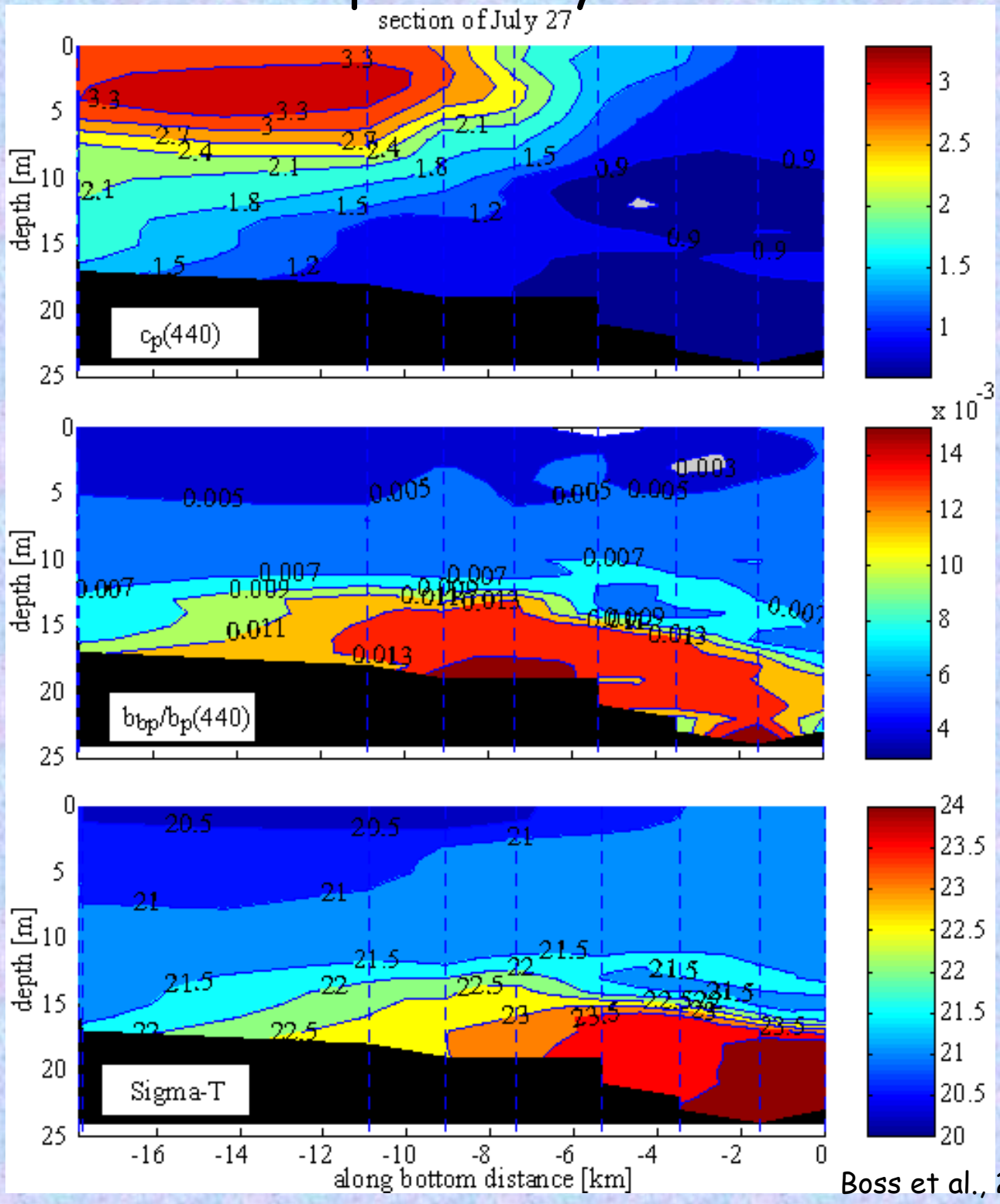

Boss et al., 200

b_{bp}/b_p is independent of concentration (surface front)

Validation by proxy:

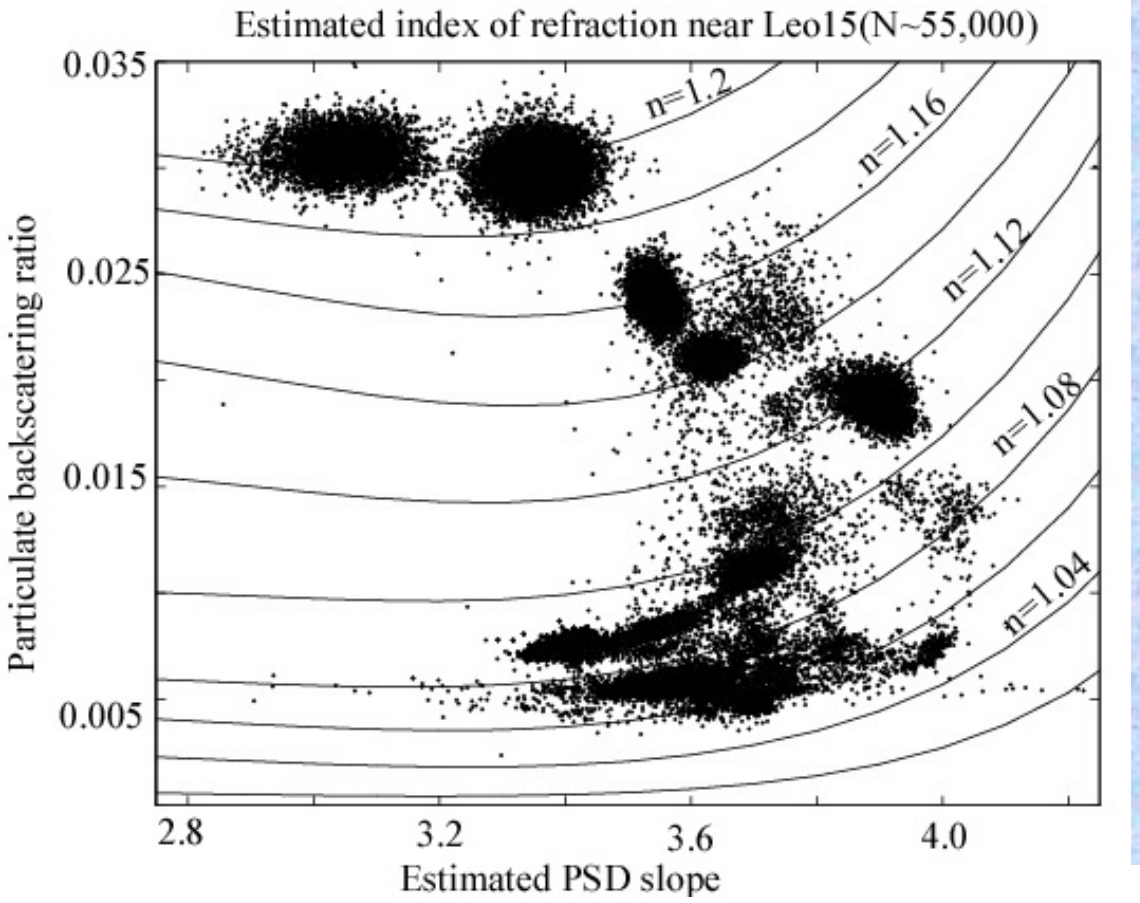

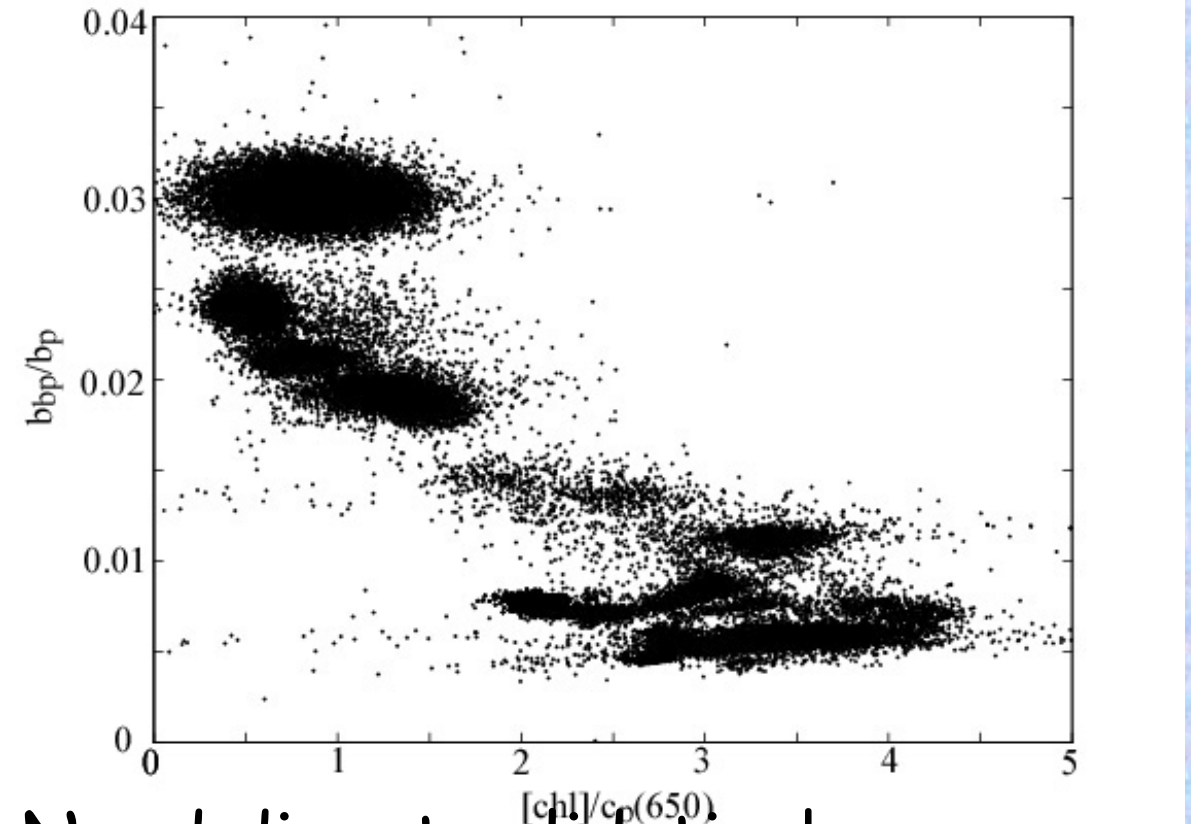

Need direct validation!

Dissolved organic matter:

CDOM, FDOM and DOC

Concentration and composition

What is colored dissolved organic matter (CDOM, FDOM)?

Operational definition:

Absorption/fluorescence by fraction smaller than:

1.0.2μm

2.0.44μm (GFF)

3.0.7μm

Currently most Ocean Optics applications use 0.2μm filters.

Absorption characteristics:

$$a_{CDOM} = a(\lambda_0)\exp(-s(\lambda - \lambda_0))$$

$$0.02 \geq s \geq 0.01 nm^{-1}$$

Consistent with measurements from the UV (280nm) to the red (660nm), though different slopes are found for different regions of the same spectra.

Believed to be due to carbon's conjugated (π) bonds in organic compounds (Shifrin, 1988).

The smaller the length of the molecule the smaller the wavelength of the light absorbed.

FDOM and CDOM:

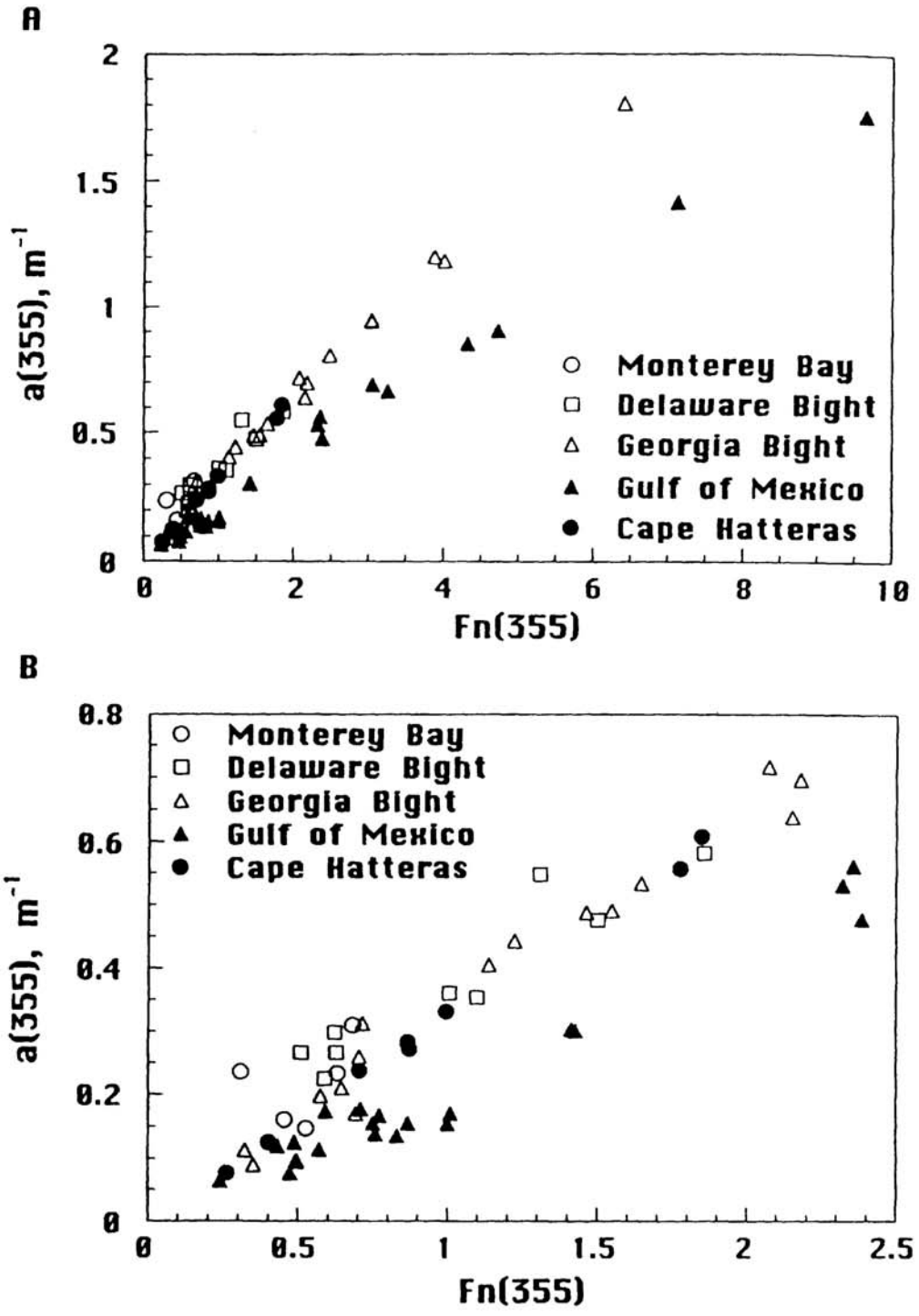

Figure 3.8 A: Relationship between the absorption coefficient at 355 nm ($a(355)$) and the fluorescence stimulated by 355 nm excitation (Fn(355)) for waters from five oceanic study sites. B: Same as Figure 3.8A, but with an expanded scale. Data from Hoge et al. (1993).

Blough and Green, 1995

Fluorescence characteristics, excitation-emission matrices:

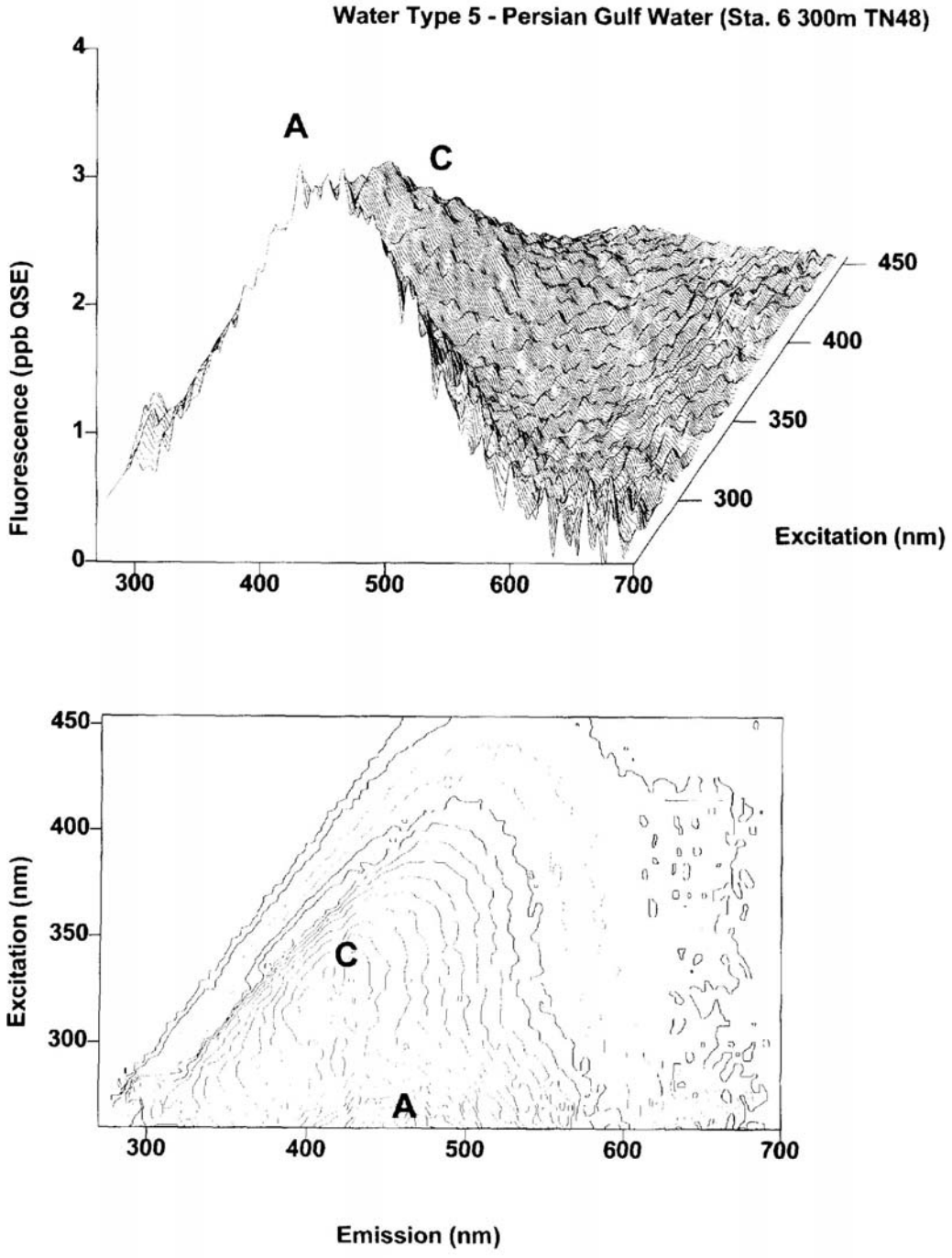

Fig. 5. Fluorescence fingerprint representative of water collected from the subsurface salinity maximum (Water Mass Type 5, Persian Gulf Water). This fingerprint is representative of most intermediate water samples.

Different peaks are associated with different families of compounds → compositional information.

DOC and CDOM:

Table 3.1 Values of $a(450)^*$ [L (mg org. C)$^{-1}$ m^{-1}] and S [nm^{-1}] for CDOM from various sources.

Source/Type of CDOM	$a(450)^*$	S	Reference
Soil Humic Acid – mean values	1.76 ± 0.21	0.0102 ± 0.0002	Zepp and Schlotzhauer (1981)
Soil Fulvic Acid – mean values	0.80 ± 0.15	0.0138 ± 0.009	Zepp and Schlotzhauer (1981)
Freshwater Aquatic Humus – mean values	0.71 ± 0.26	0.0145 ± 0.0017	Zepp and Schlotzhauer (1981)
Suwanee River Humic Acid[1]	1.57[2]	0.0120	This paper
Suwanee River Fulvic Acid[1]	0.51[2]	0.0161	This paper
Orinoco River CDOM[3]	1.23 ± 0.09	0.0141 ± 0.0008	Blough et al. (1993)
Gulf of Paria CDOM[3]	0.65 ± 0.06	0.0145 ± 0.0004	Blough et al. (1993)
Marine Fulvic Acid			
Mississippi Plume	0.007 ± 0.001	0.0194 ± 0.00044	Carder et al. (1989)
Gulf Loop Intrusion	0.005 ± 0.001	0.0184 ± 0.00166	Carder et al. (1989)
Marine Humic Acid	0.1302 ± 0.00005	0.0110 ± 0.00012	Carder et al. (1989)
Marine Aquatic Humus – mean values	0.33 ± 0.09	0.0147 ± 0.0006	Zepp and Schlotzhauer (1981)
Sedimentary Fulvic Acid Molecular Weight			
< 10,000	0.093	0.0183	Hayase and Tsubota (1985)
10,000–50,000	0.109	0.0181	Hayase and Tsubota (1985)
50,000–100,000	0.195	0.0157	Hayase and Tsubota (1985)
100,000–300,000	0.386	0.0125	Hayase and Tsubota (1985)
> 300,000	0.317	0.0130	Hayase and Tsubota (1985)

[1] International Humic Substances Society standard.
[2] Calculated assuming that this material contains 50% C by weight.
[3] Collected by solid phase extraction on C18 reversed phase cartridges.

Blough and Green, 1995

DOC-specific CDOM absorption is bounded and is nearly constant in a given coastal environment:

7 different rivers in Georgia

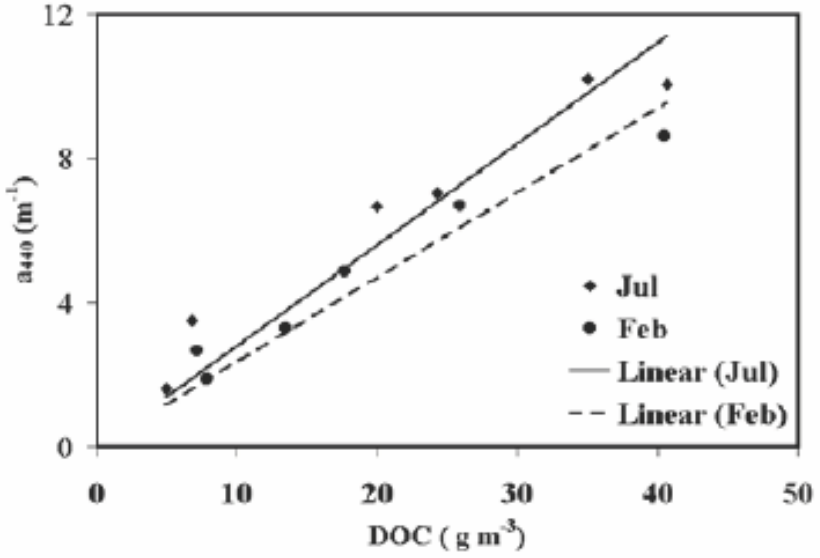

Fig. 2. A plot of the absorption coefficient at 440 nm *versus* DOC concentration in the origin samples. The relationship between the two parameters was: y = 0.2796x (r^2 =0.9051, n = 6, p <0.0007) in July 1999, and y = 0.2352x (r^2 =0.9210, n = 6, p <0.0005) in February 2000.

Yakobi et al., 2003

Link between DOC, molecular weight and spectral slope of CDOM:

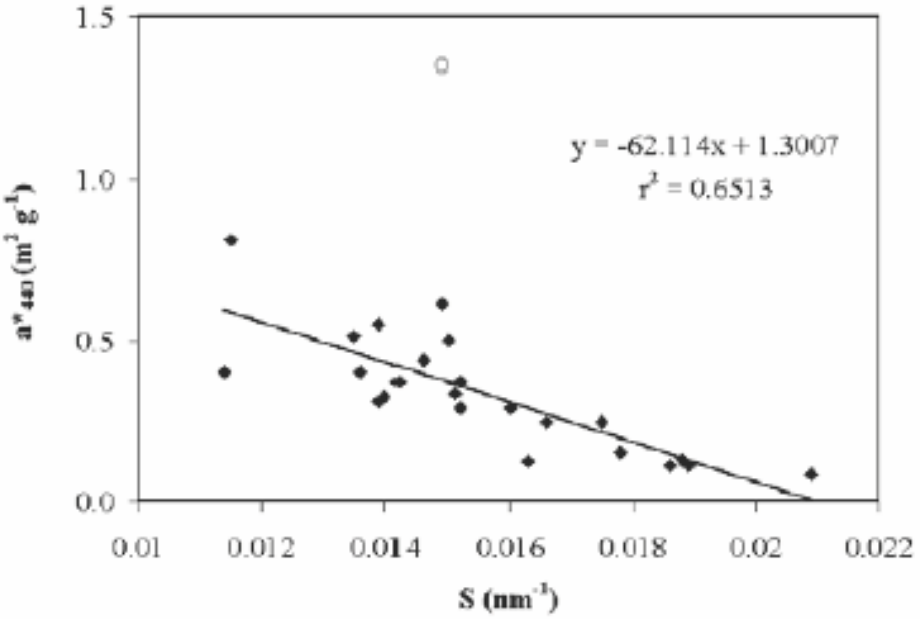

Fig. 4. A plot of slope coefficient, S, *versus* specific attenuation coefficient, a^*_{440}. All samples and fractions of the July 1999 survey are included. The variables measured on the Altamaha large fraction sample (○) were excluded from the calculation of the regression line. The relationship of the 2 parameters in February 2000 was: a^*_{440} = -69.034*S+1.3, r^2 = 0.72, n = 22, p <0.001.

Fraction	Large	Medium	Small	Origin
	(S, nm^{-1})			
July 1999				
Suwannee	0.0146	0.0175	0.0209	0.0166
Ogeechee	0.0139	0.0152	0.0186	0.0152
Satilla	0.0150	0.0142	0.0188	0.0160
St Marys	0.0149	0.0136	0.0178	0.0151
Altamaha	0.0149	0.0114	0.0189	0.0135
Savannah	0.0115	0.0139	0.0163	0.0140
av	0.0141	0.0143	0.0186	0.0151
std	0.00135	0.00201	0.00151	0.00117
cv	9.6	14.0	8.1	7.8
February 2000				
Suwannee	0.0154	0.0175	0.0201	0.0172
Ogeechee	0.0136	0.0164	0.0169	0.0160
Satilla	0.0130	0.0157	0.0175	0.0162
St Marys	0.0140	0.0156	0.0181	0.0163
Altamaha	0.0108	0.0151	0.0148	0.0142
Savannah	0.0116	0.0159	0.0169	0.0156
av	0.0131	0.0160	0.0174	0.0159
std	0.00167	0.00083	0.00173	0.00099
cv	12.8	5.2	10.0	6.2

Yakobi et al., 2003

S- linked to molecular weight using ultra-filtration

Example: pore water measurements:

Flood tide:

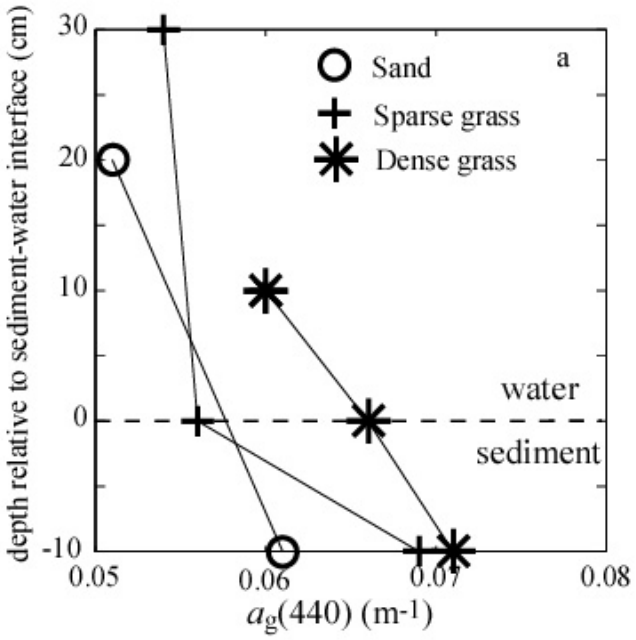

Ebb tide:

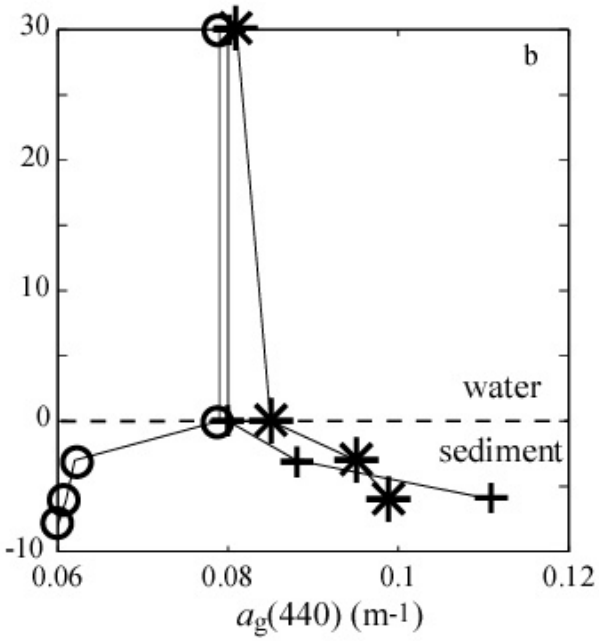

Boss and Zaneveld, 2003

CDM (CDOM+NAP) from Ocean Color:

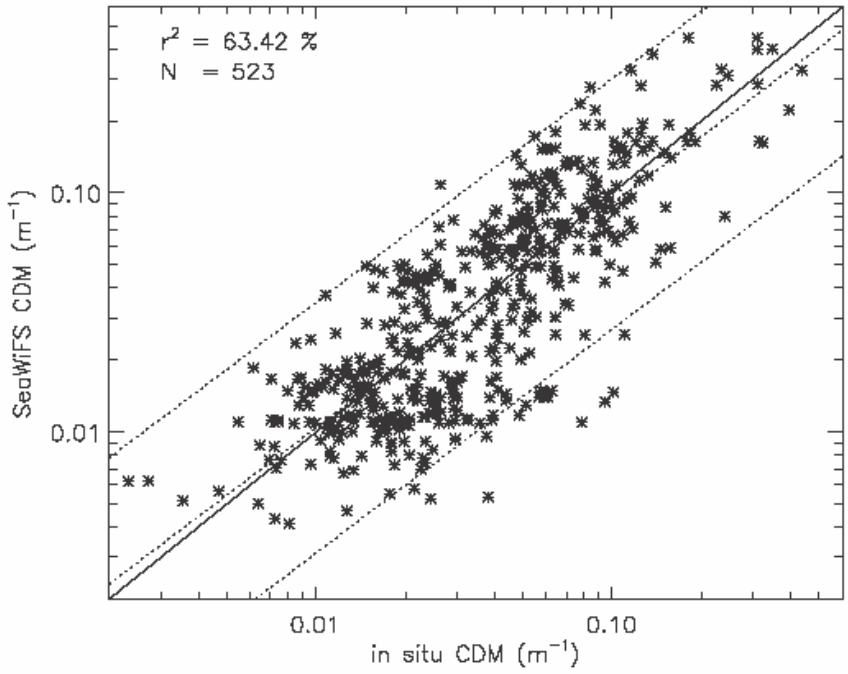

Figure 1. Comparison of near-simultaneous SeaWiFS and in situ CDM observations from around the world ($N = 523$). The match-up procedure is described in the text. The r^2 value for the log-transformed CDM estimates is 63.42%, and the fit power law relation is (SeaWiFS CDM) = 0.775(in situ CDM)$^{0.935}$ (the middle dotted line). The outer dotted lines represent the 95% confidence interval for the fit, and the solid line is the 1:1 line.

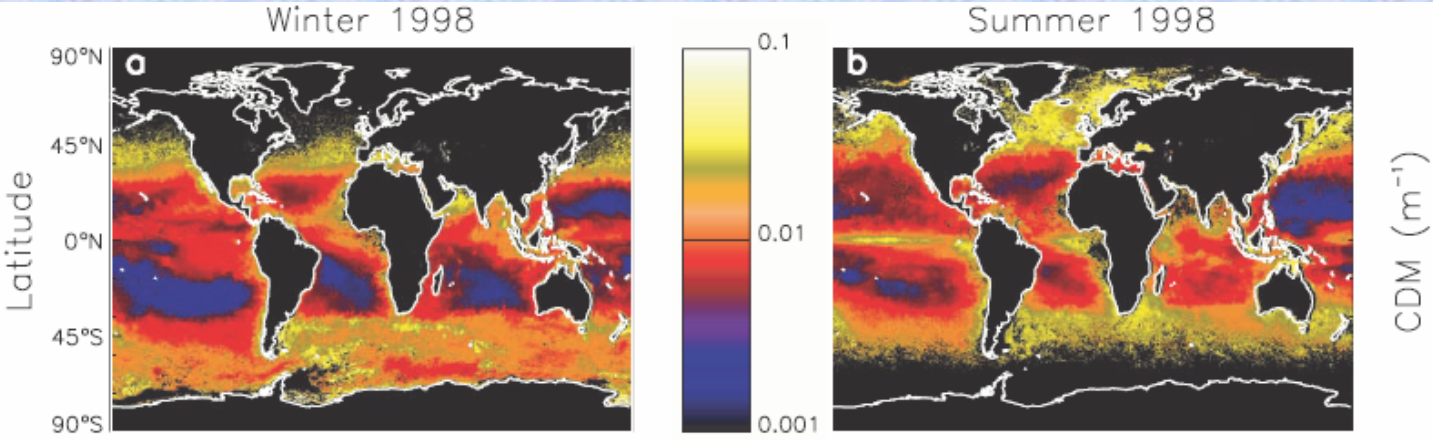

- CDM has been found to be correlated with a_ϕ, suggesting contamination (Siegel et al., in press).
- UV bands should improve retrievals and possibility of separating CDOM and NAP absorption

Inversion to obtain rate processes:

I. Fluxes of particulate and dissolved materials:

Combine high-frequency measurements of concentration proxies with 3-D velocity to compute eddy correlation:

Vertical eddy flux=<w'[conc.]'>
Fugate and Friedrichs, 2002

Average settling velocity:
W_s= =<w'[conc.]'>/{d<[conc.]>/dz}
Fugate and Friedrichs, 2002

Problem: biased to sizes the ADV is sensitive to.

II. Phytoplankton growth rate:

a. Direct Lagrangian measurements (D'Asaro).

b. $\mu=\mu$ (E_d,Temp.Nut,[chl],C_{phyto})

Based on the works of Geider, McIntyre, & Sakshaug {Behrenfeld et al., 2004, GBC}.

Problem: currently assumes balanced growth.

Direct measurement of growth (D'Asaro)

ML float:

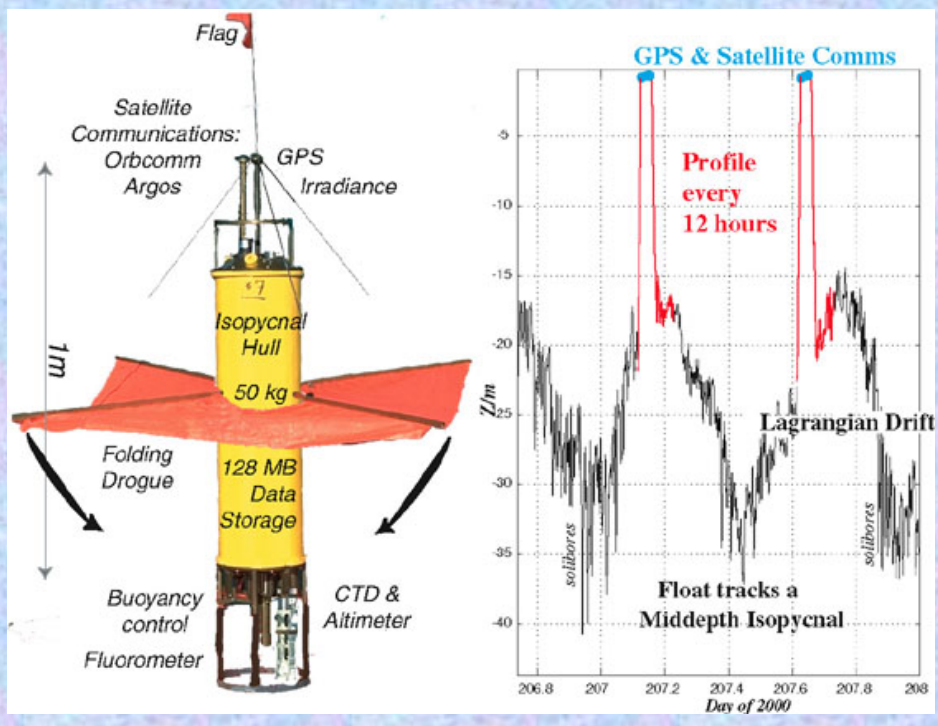

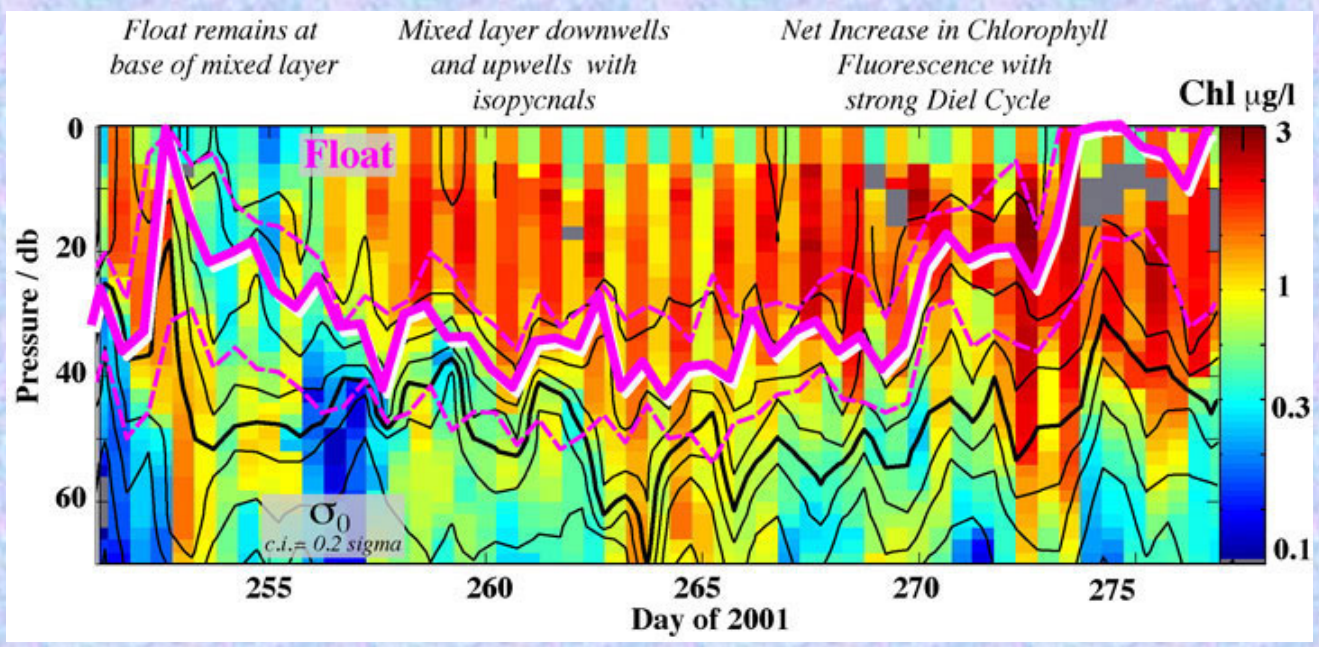

Direct measurement of growth (D'Asaro):

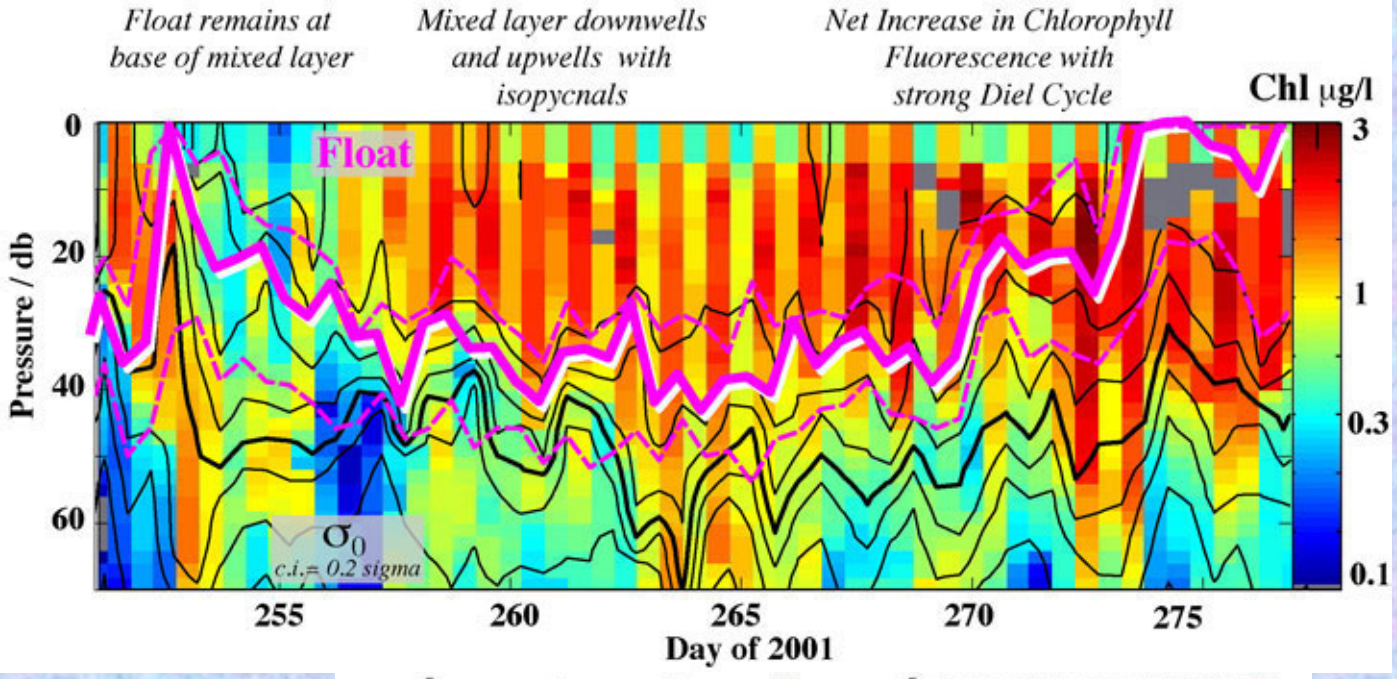

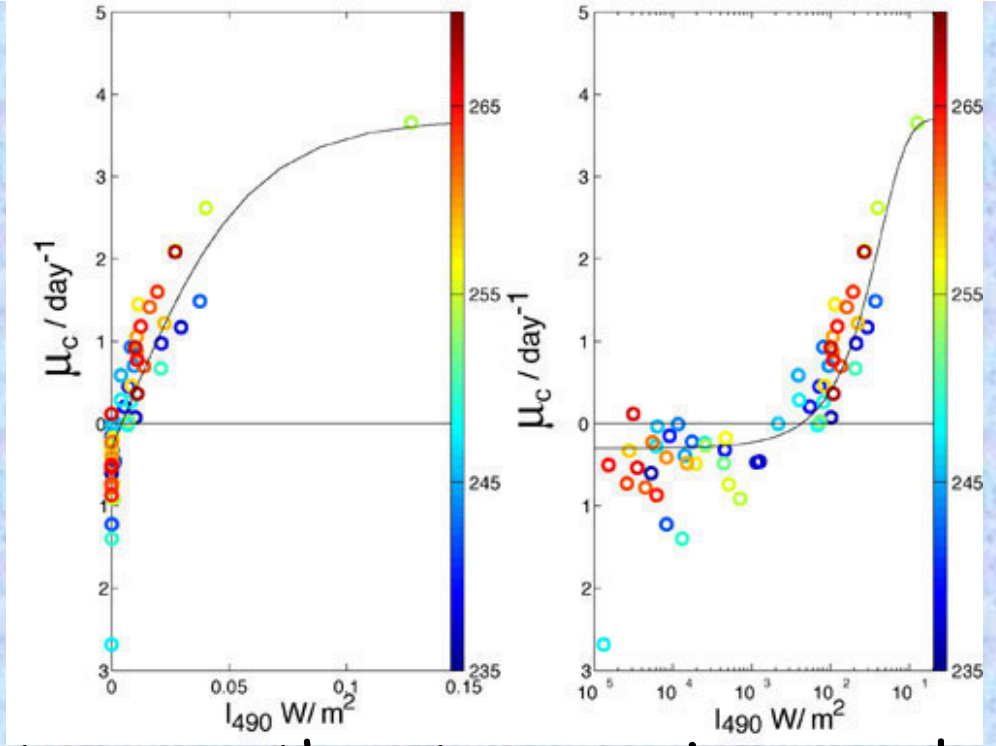

Phytoplankton growth-rate on an isopycnal:

μ_c=1/[chl]xD([chl])/Dt

Based on averages in a 12hrs trajectory

A novel approach to obtain PP information

Getting independently [chl] and C_{phyto} is exciting because:

If one knows E, [chl]/C_{phyto}, & Temp. → phytoplankton growth rate.

A hint at that was seen in the following data sets:

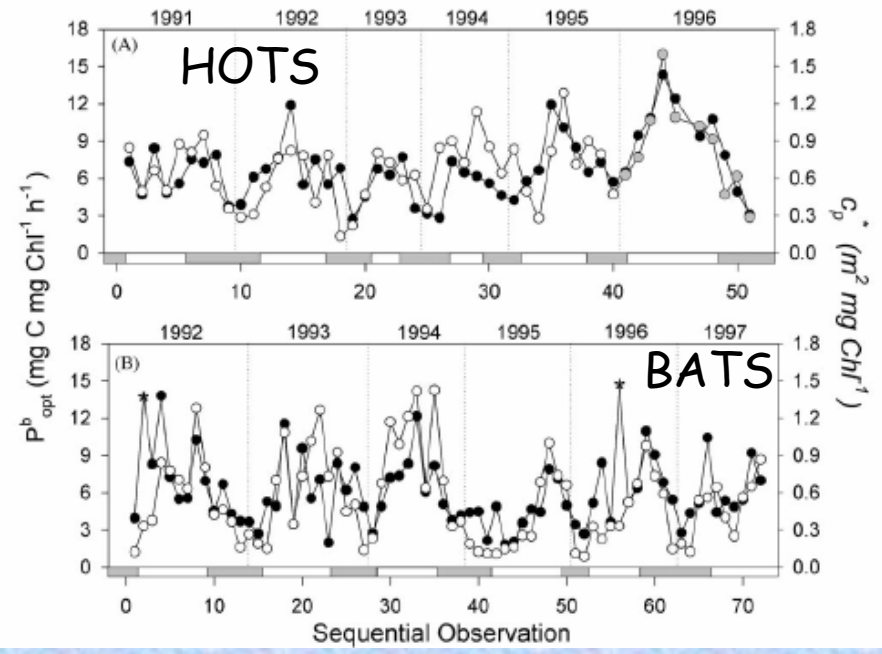

OliPac

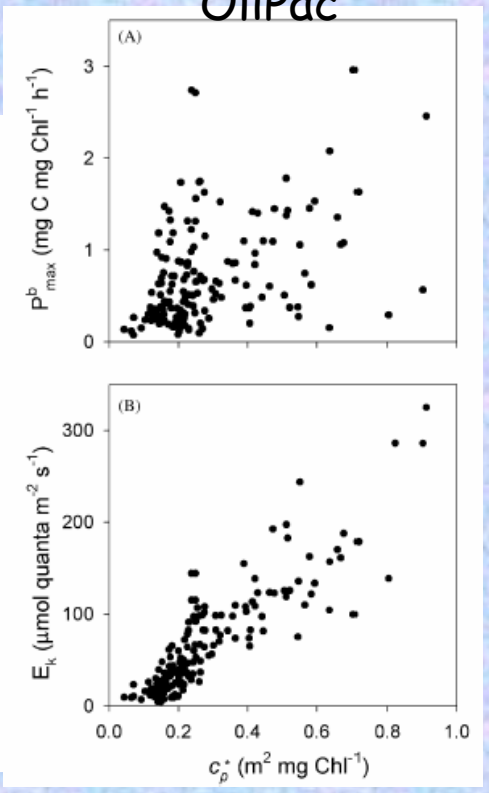

Behrenfeld and Boss, 2003, DSR I

→ $\frac{c_p}{[chl]}$ **is correlated with physiological variables**

Obtaining μ from space (Behrenfeld et al.):

1. Retrieve b_{bp} and [chl] from space
2. Compute: $\text{phytoplankton C} = 13{,}000 \cdot (b_{bp} - 0.00035)]$
3. Obtain ML light, $I_g = I_0 \exp(-k_{490} MLD/2)$
4. Derive maximal chl/C for given T, I_g, and plenty of Nuts.
5. Assume growth decrease proportionally with reduction of chl/C relative to its maximal value:

$$\mu = \mu_{\max}\left(1-\exp\left(-3I_g\right)\right)\frac{chl/C}{chl/C_{N,T-\max}}$$

$$chl/C_{N,T-\max} = 0.022 + \left(0.045 - 0.022\right)\exp\left(-3I_g\right)$$

6. Divide the globe to 28 regions based on variability in [chl] and geography and observe averaged annual cycle.
7. Compute NPP: $\mathrm{NPP} = \mathrm{C} \cdot \mu \cdot \mathrm{Z_{eu}} \cdot h\,(\mathrm{I_o})$

Obtaining C_{phyto} and [*chl*]/C_{phyto} from space

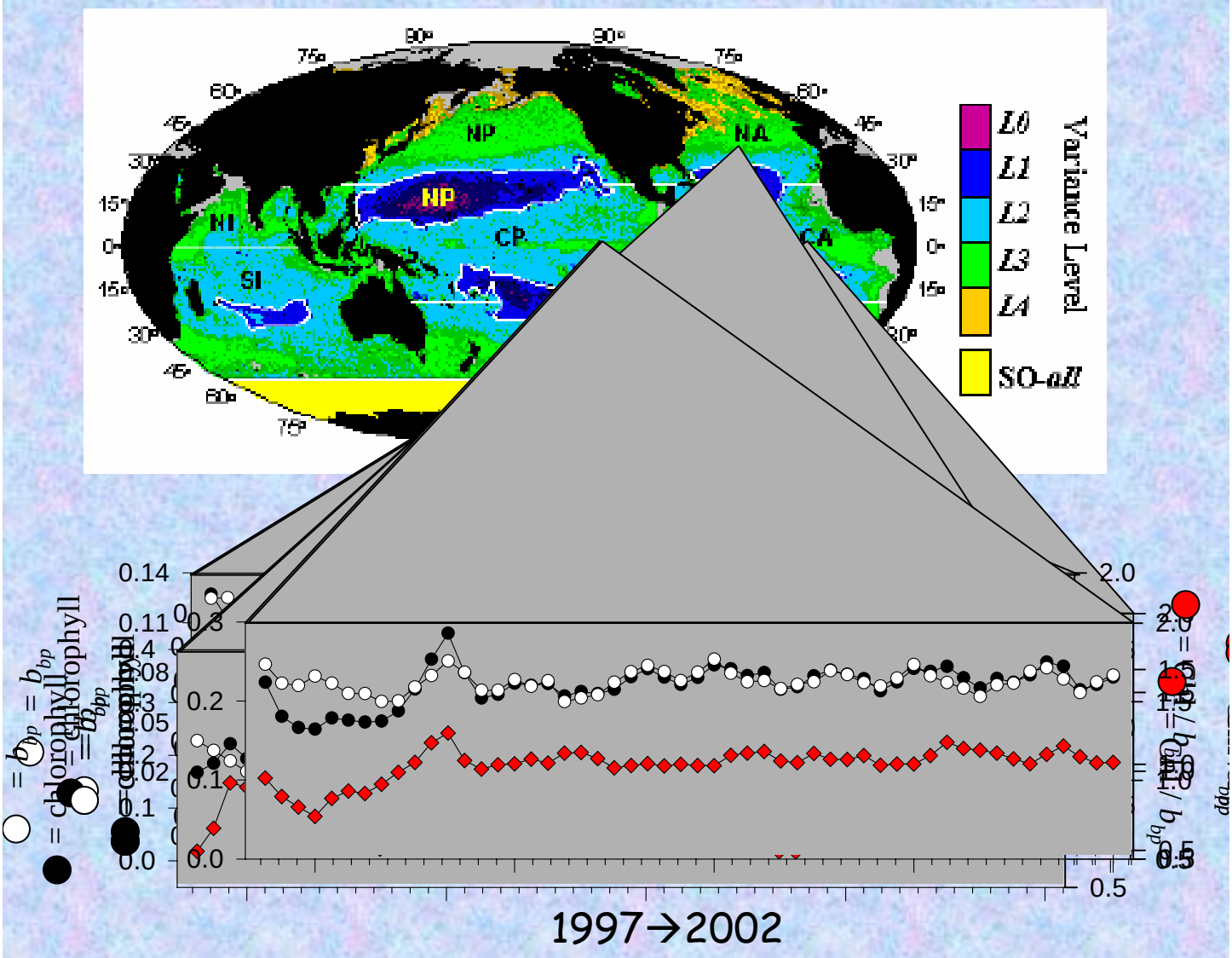

28 different regions based on ocean basins and 5 groups of variability in [*chl*]

An equation relating [chl]/C_{phyto} and light (e.g. Cloern, 1995):

$$\frac{[chl]}{C_{phyto}} = \left.\frac{[chl]}{C_{phyto}}\right|_{\min} + \left\{\left.\frac{[chl]}{C_{phyto}}\right|_{\max} - \left.\frac{[chl]}{C_{phyto}}\right|_{\min}\right\} \exp\left[-\frac{I_g}{I_{ref}}\right]$$

I_g = the regional monthly median ML light level and I_{ref} = 1/3 moles photons m^{-2} h^{-1}. ML is provided from the Navy's model.

$\left.\frac{[chl]}{C_{phyto}}\right|_{\max}$

$\left.\frac{[chl]}{C_{phyto}}\right|_{\min}$

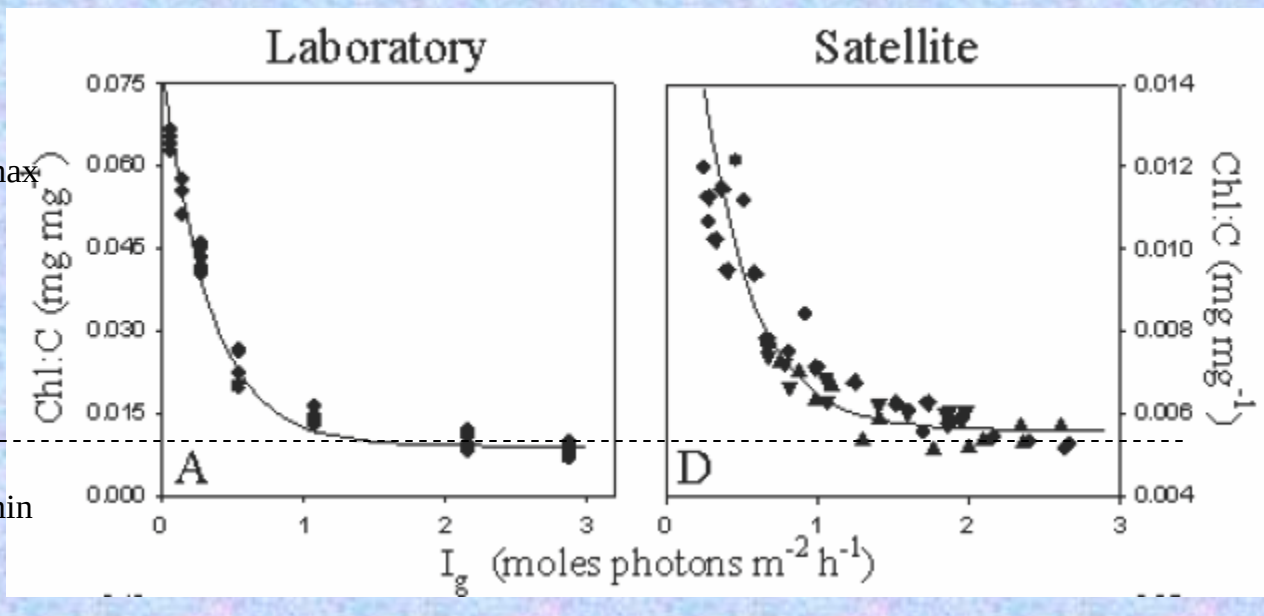

Furthermore, $\left.\frac{[chl]}{C_{phyto}}\right|_{\min\ \&\ \max}$ have well characterized responses:

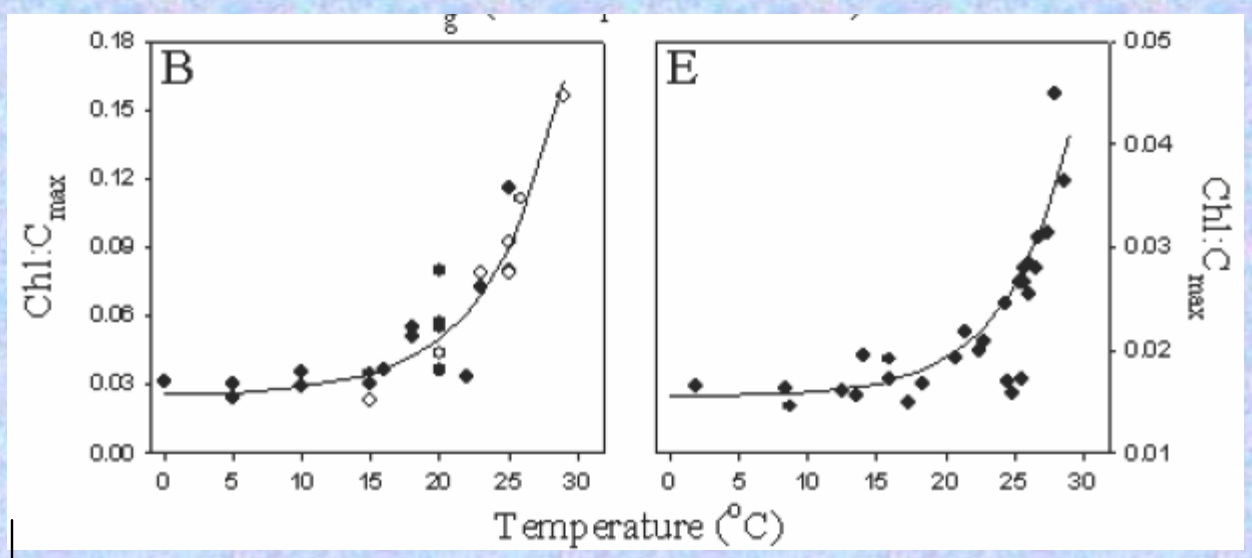

$\left.\frac{[chl]}{C_{phyto}}\right|_{\max,SAT}$ increases with temperature, similar to its *temperature dependence* in cultures.

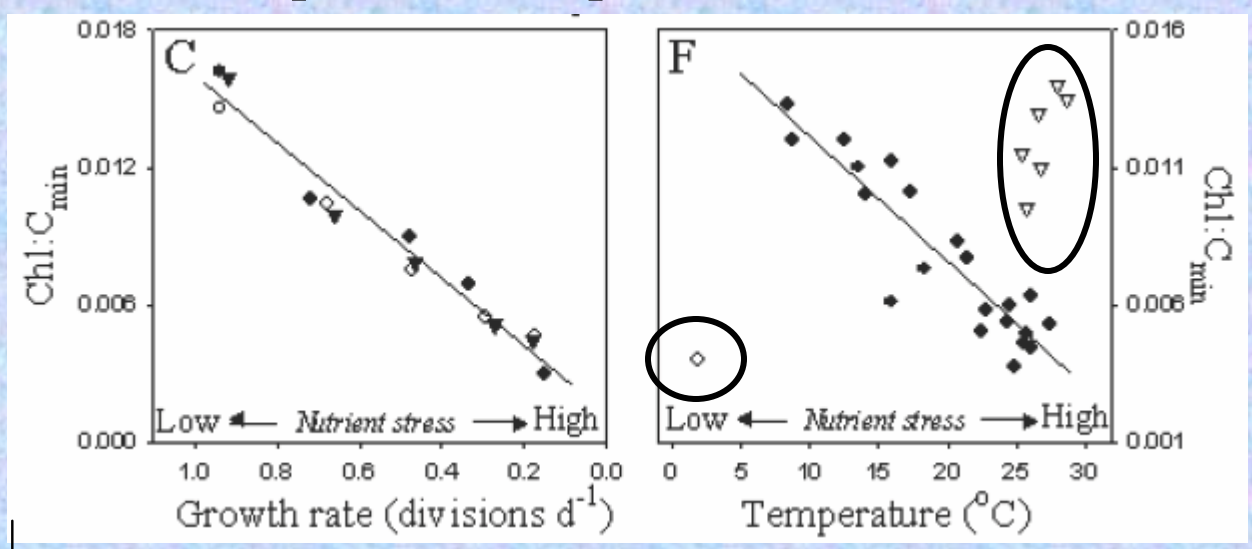

$\left.\frac{[chl]}{C_{phyto}}\right|_{\min,SAT}$ decreases with temperature in all the parts of the oceans where temperature is indicative of *nutrient stress*.

Estimates if μ from space:

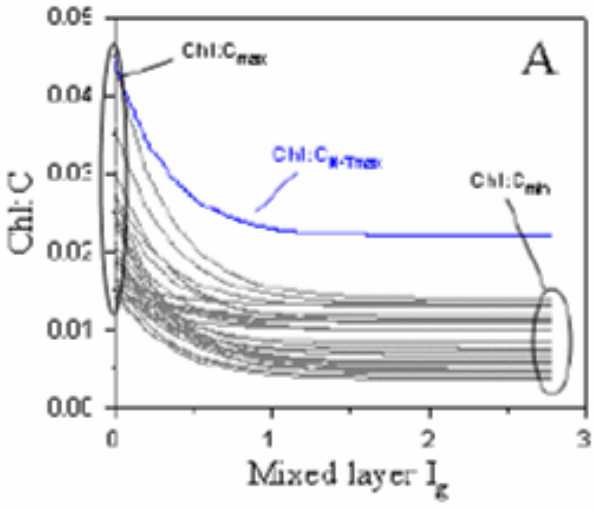

summer

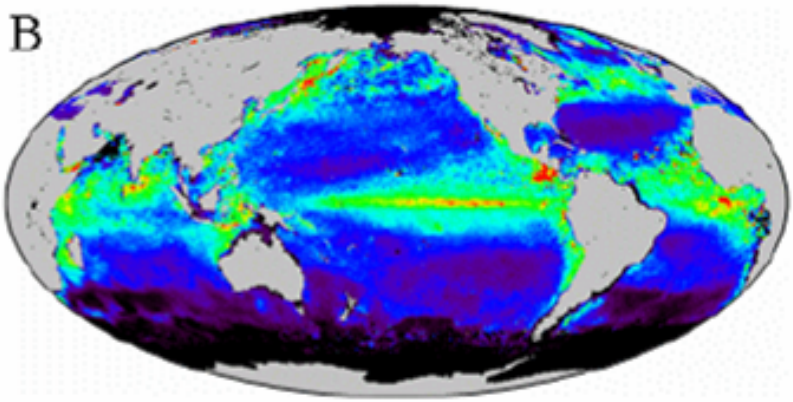

winter

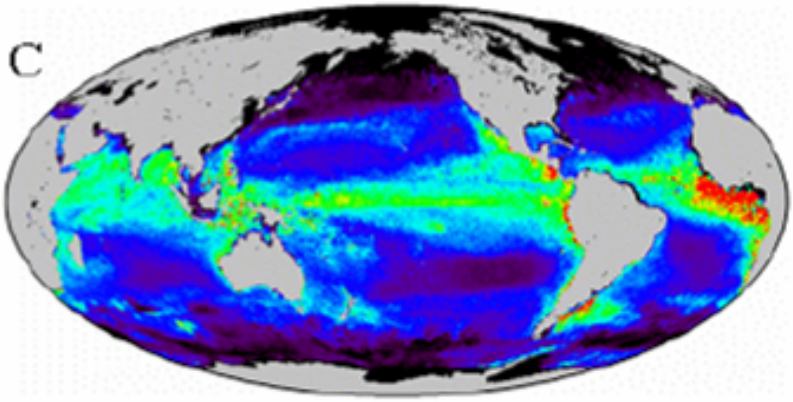

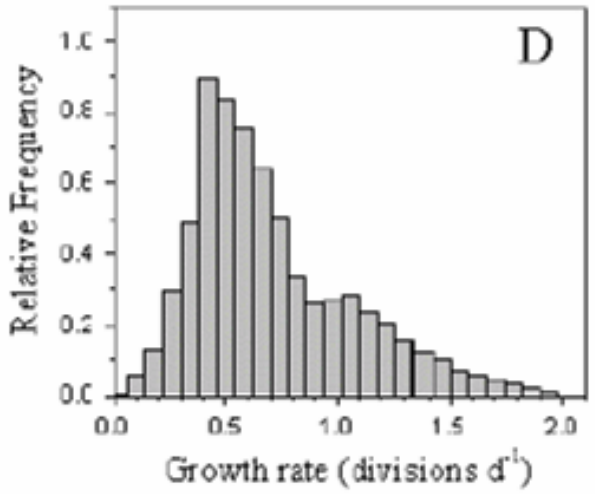

Needs independent validation!!

Comparison with a current model (VGPM):

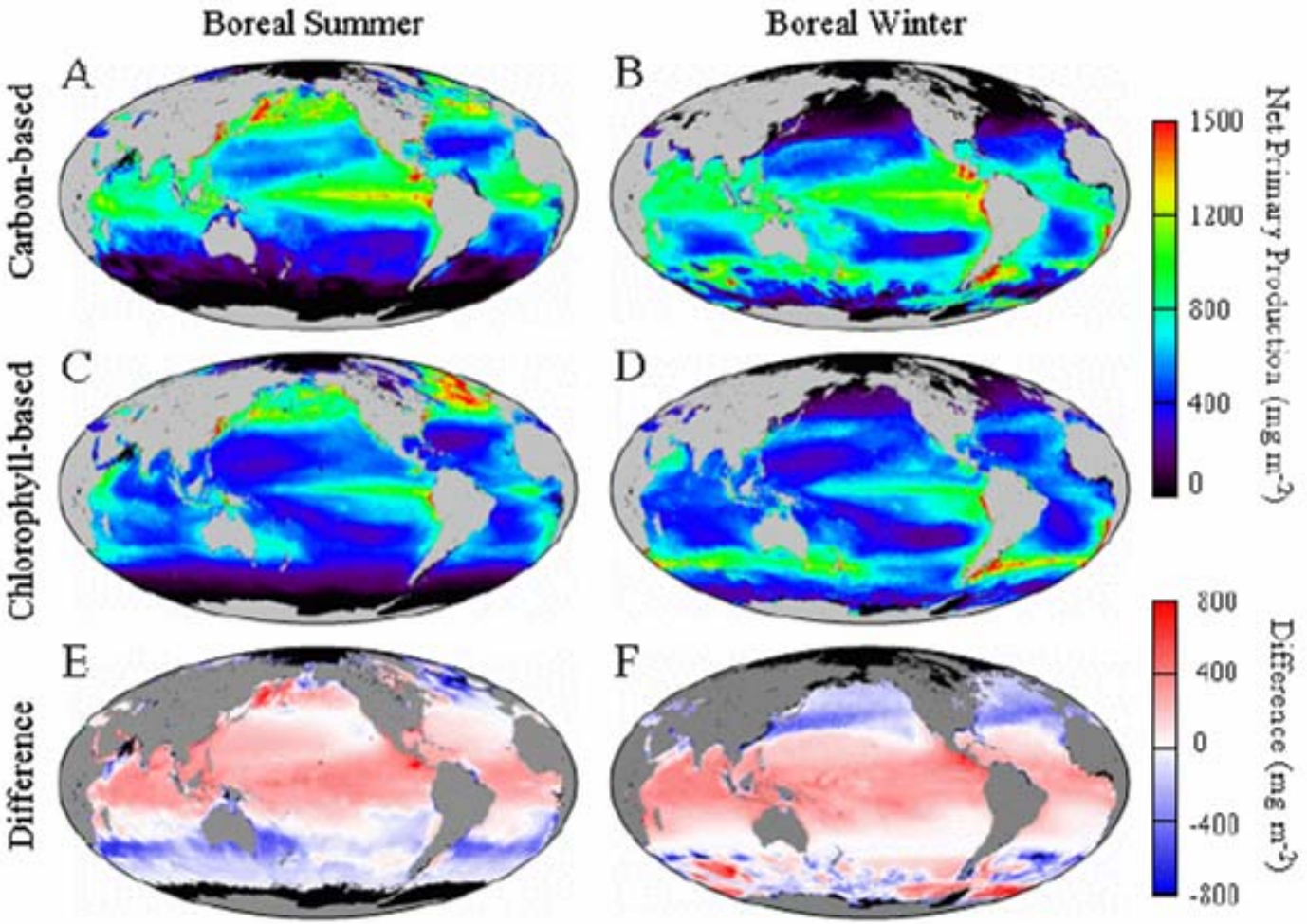

Significant regional differences. Difference in timing:

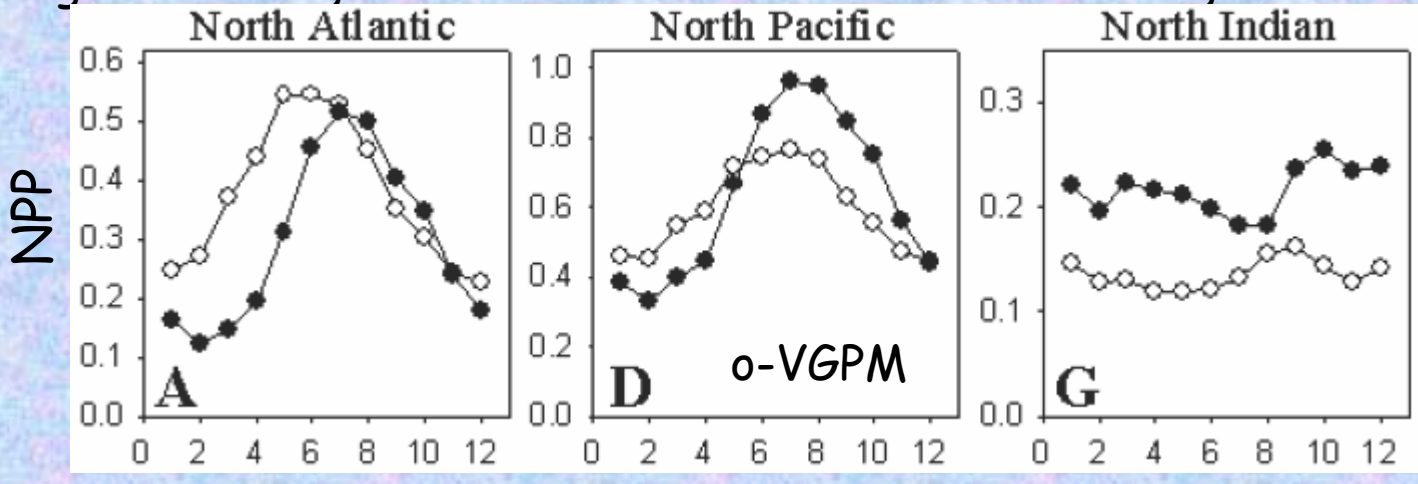

Many aspects need improvement:

- Move from [chl] to a_ϕ.
- Balanced growth assumption.
- C_{phyto}: effects of size and ecology.
- Inorganic particles.

Food for thought:

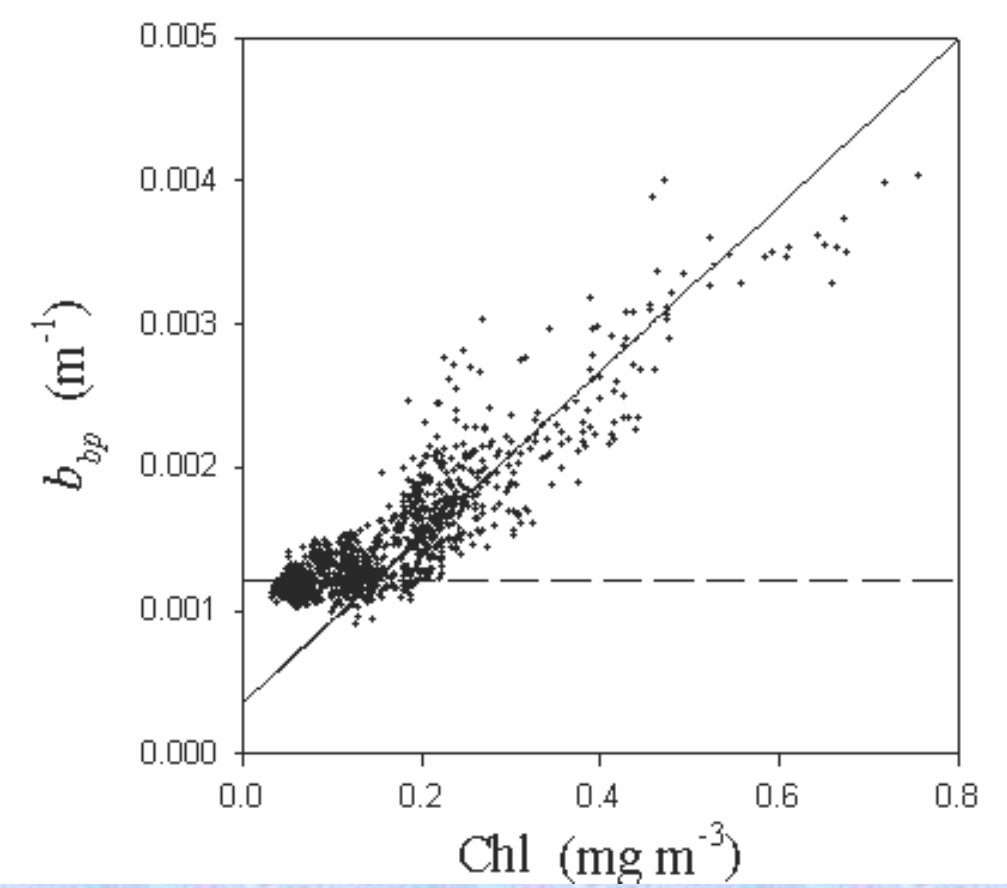

In low biomass waters, [chl] seems a poor proxy of C_{phyto}.